Flugmælingar og úttekt á loftkviku yfir Hvassahrauni

- Viðaukar -

Verkefnistími: janúar 2021 – mars 2024

Verkefnisstjórar:

Gylfi Árnason

Þorgeir Pálsson

Ólafur Rögnvaldsson

Sæmundur E. Þorsteinsson

Table of Contents

# Appendix A: Visualization of In-flight Measurements.

To explain the data processing and how information can be extracted from the measurement data we go through the processing of measurements from 2022.06.17. Data was collected by three aircraft simultaneously (TF-VTR ICP Ventura, TF-SRO and TF-MET both ICP Savannah). We process each flight individually, and then combine all three. First we look at TF-MET and examine the track with the help of Google Earth (fig 1). The red circle with radius 10 km (6 NM) has its midpoint in the assumed middle of the planned airport. The track is green, and EDR along the track is shown at the bottom. The track can be followed with a pointer and EDR and other data can be read from the track and compared to geographical features that may be suspect for generating some of the measured turbulence. In this case with Easterly wind the highest EDR occurrences are close to the hills in the SE part of the circled area.
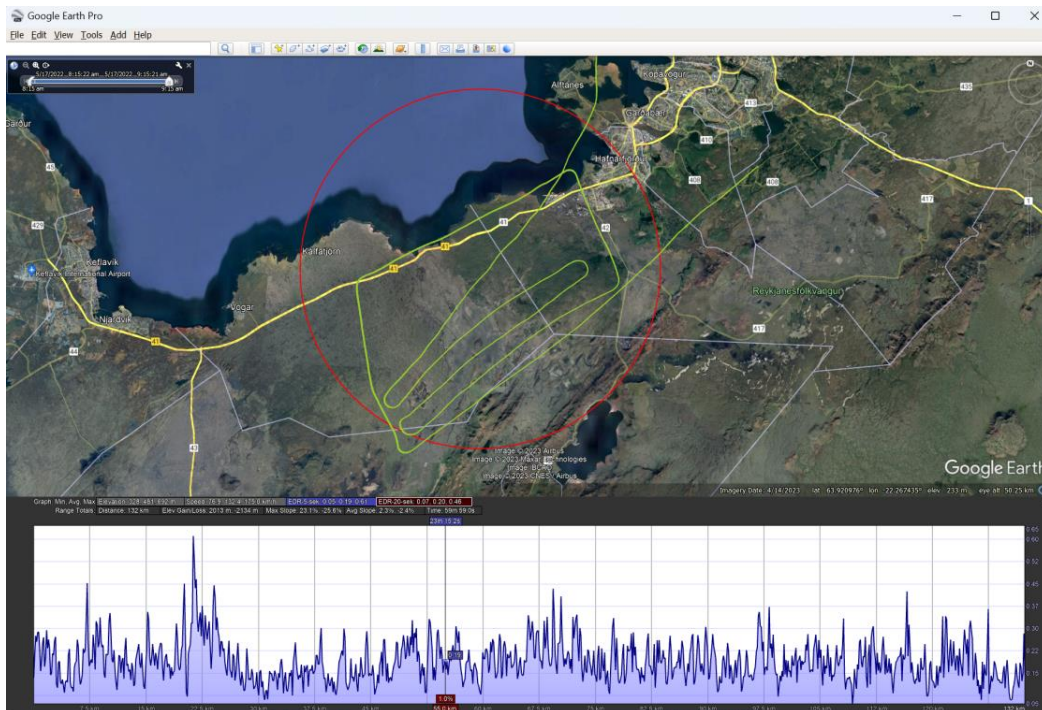
In fig 2 we have another view of the track demonstrating RMS g plots with rolling 1s, 5s and 20s time averages. The horizontal line at 1 m/s^2 marks the onset of light turbulence for most aircraft.
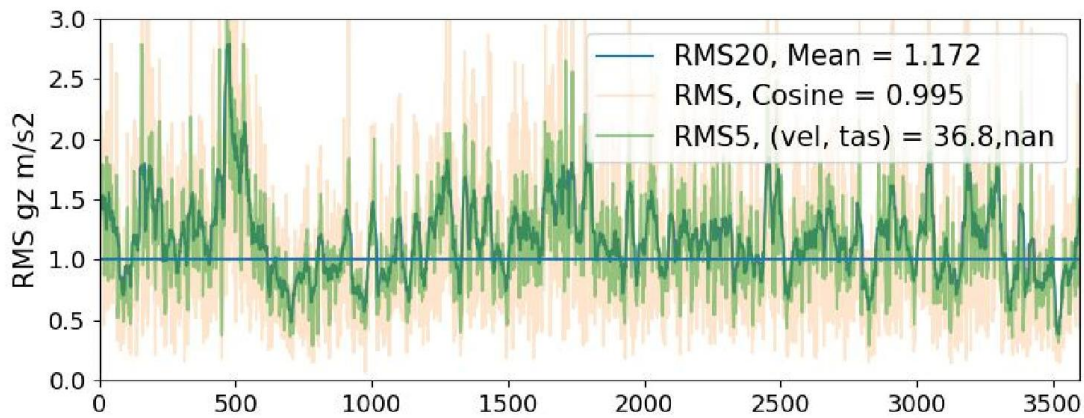
Another way to visualize (fig 3) the track is to color code the EDR value as demonstrated here (a), where darker color indicates higher EDR. The location data (GPS) has been converted to local km coordinates based on the assumed midpoint of the planned airfield. Further, a colored point chart (b) is calculated by interpolating data from the track to a 50x50 grid (spanning 20x20 kilometers). We then add contour lines (c) and fill with color for the final picture (d), which now helps with visualizing the distribution of EDR in the area.
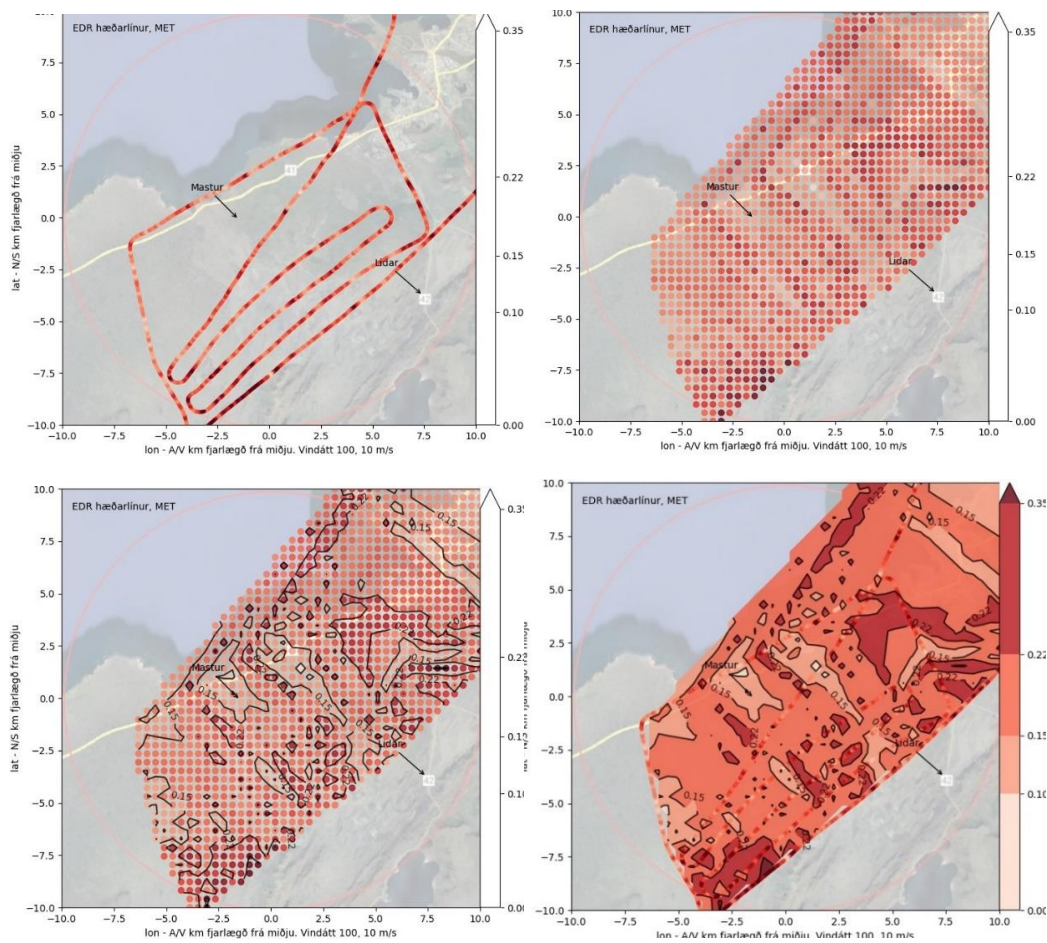
The following sheet is generated for quality control after each measurement trip. It includes some spectral analysis, compares data to the -5/3 slope and more. The conversion from vertical acceleration to EDR is displayed along with various other details that help evaluate the results from the measurement track. Wind speed and direction (as measured by the mast in the area) are also displayed. On this particular day we were using three aircraft (assigned 1400ft ASL, 500ft AGL, and 2000ft ASL) simultaneously for measurements. Each one with an independent track generating a quality control result sheet displayed below (fig 4).

The tracks now span various heights in the area, this allows for a 3D interpolation (similar to the above 2D or horizontal interpolation). We use 50*50*20 grid with height spanning from 150 m to 650 m ASL. To visualize the 3D results we plot 4 horizontal sections and add two vertical sections (see fig 5).
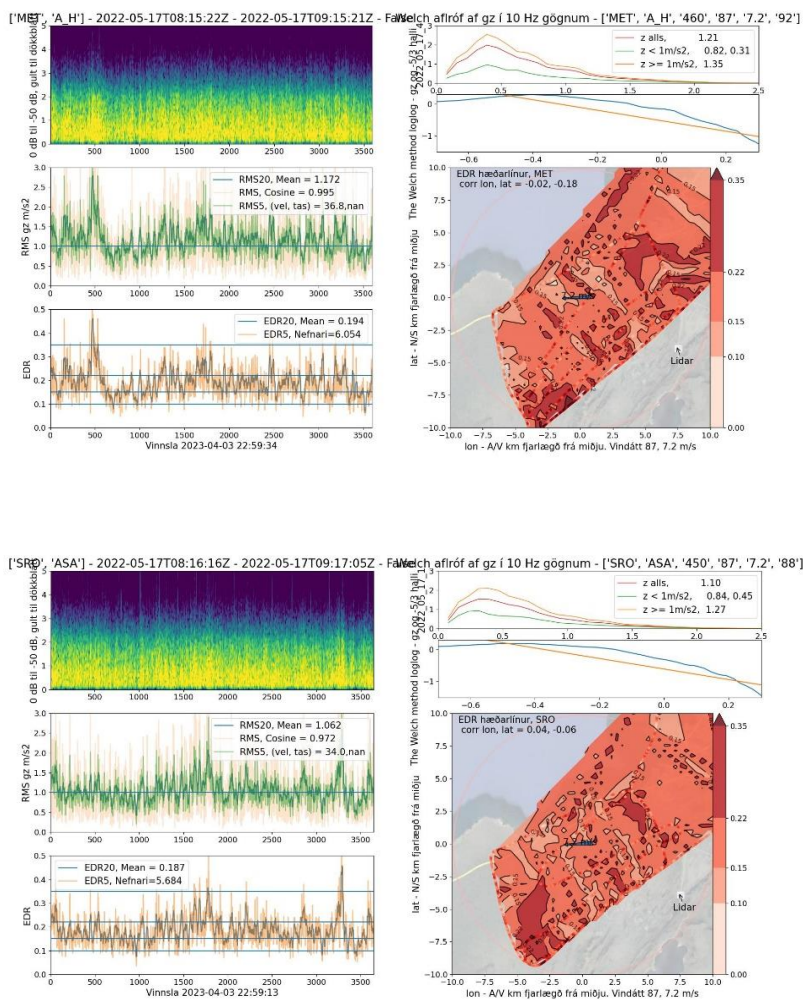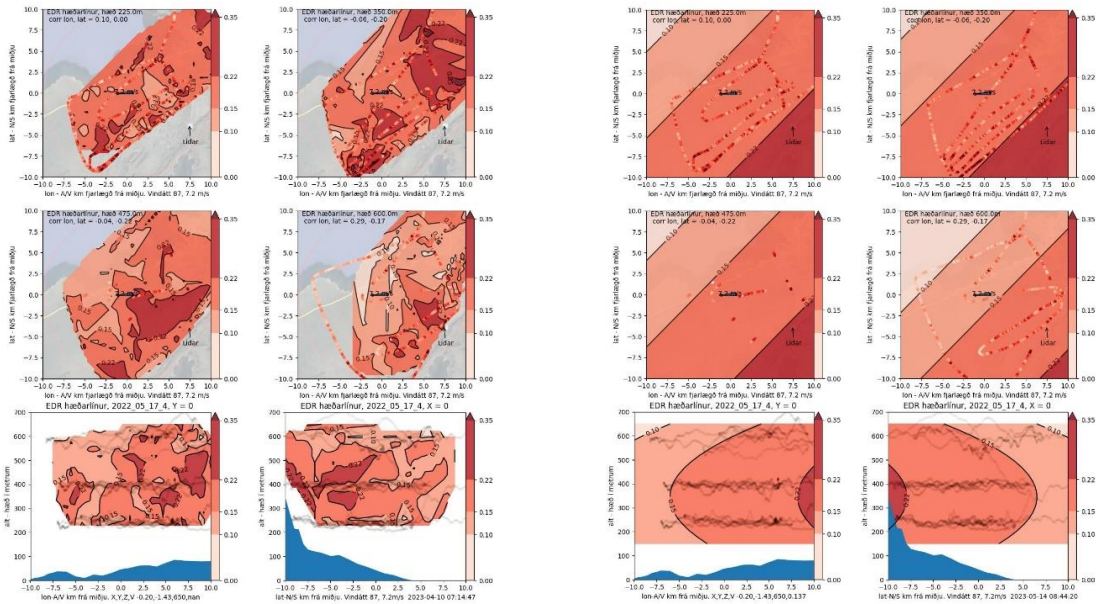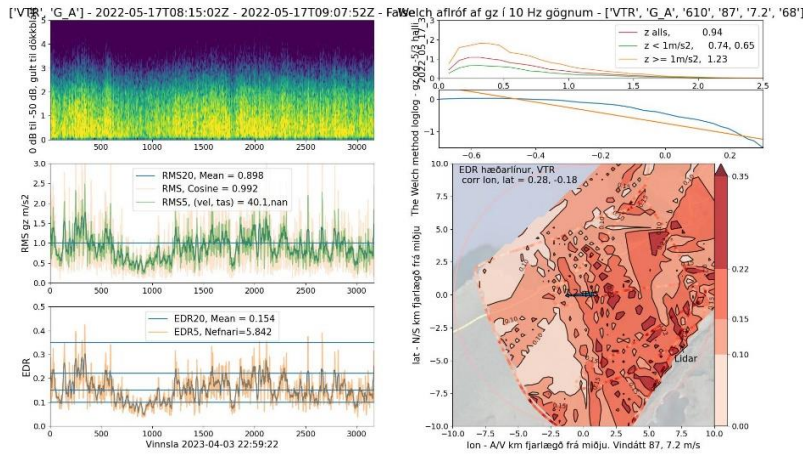
This way of visualizing the results filters out some of the measurement details which are thus lost in the interpolation process. Extreme measured values are smoothened with results from close by points before display. There is a compromise between seeing the details or seeing an overall picture.

Another approach to gaining an overall picture of the distribution of EDR in the area of interest is to do a multilinear curve fit. In this case we choose x (lon), y (lat), and h (alt) as the independent variables and EDR as the dependent variable. We input alt as a parabola to allow for maximum or minimum in EDR with height. The curve fitted is thus;

EDR = a***lon**+b***lat**+m*(**alt**-n)**2+e = a***lon**+b***lat**+m***alt**2-2*m*n***alt**+e

$= a*\mathbf{lon}+b*\mathbf{lat}+c*\mathbf{alt**2}+d*\mathbf{alt}+e$

The altitude of min or max EDR is therefore at n = -d/2/m

i.e. we look for the 5 parameters that minimize the error between fitted and measured EDR values. In this case the parameters are:

a,b,c,d,e = 4.93141616e-03 -4.84839655e-03 -5.38704837e-07 3.71737371e-04 1.16587838e-01

with R^2 = 0.3 (correlation coefficient of 0.55), based on around 8100 measurement points within the 10 km radius circle around the assumed midpoint of the planned airfield.

We show the visualization (fig 6) of the curve fit in the same way as 3D interpolated measurements. Readers are left with choosing a visualization method that suits their purpose best. The details in fig 6 are similar to a description by experienced pilots of distribution of turbulence on the lea side of hills, but here with quantified levels of EDR. Note that the parameter n = -d/2/m indicates a maximum in EDR at roughly 345 m ASL, which is close to the height of hills upstream from the measurement area.

We can also combine multiple measurement days with added independent variables of EDR, wind speed and wind direction from the Mast, and do a curve fit. Here we present such a collection of 23 measurement tracks where one Mast average windspeed and direction is used per track (fig 7, 8).

$= a*\mathbf{lon}+b*\mathbf{lat}+c*\mathbf{alt**2}+d*\mathbf{alt}+e+f*\mathbf{wspd}+g*\mathbf{wdir}$

with a,b,c,d,e,f,g=2.835e-03 -5.526e-03 -2.247e-07 7.240e-05 1.067e-01 3.697e-03 3.086e-04. This is based on 63000 measurents. Correlation coefficient r=0.525, average wspd is 8.4m/s and average wdir is 81 degree.
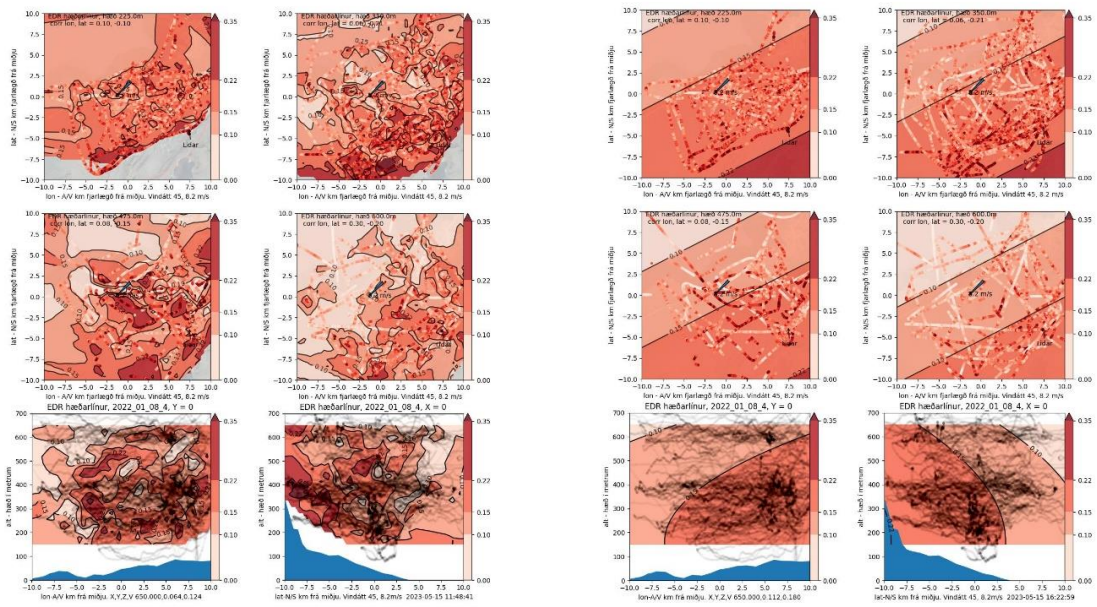
More detailed results are presented in the main report, where correlations are made with 10 minutes averages from the Mast.

Appendix B: Correlation Model

The following document presents a model of in-flight EDR (Eddy Dissipation Rate) calculation using a 5-second (and 20s) running window over a specific area of interest. The model incorporates various flight variables and ground mast observations. Its key components consist of spatial factors, namely latitude and longitude (represented in km from midpoint), and altitude (m ASL), as well as atmospheric factors, specifically windspeed (m/s) and direction (degrees). Notably, to improve the accuracy in capturing orographic turbulence, which is elaborated in detail in the main report, the altitude factor of the model incorporates an inflection point, allowing for a maximum value at a particular height.

Given that the aircraft used in the study were not equipped to measure windspeed and direction during flight, results from a weather mast were used to obtain representative values for the entire area of interest in the modeling process. This approach of modeling local details could be valuable in developing a methodology for estimating local low-level turbulence over and around airports with airport weather masts.

The dataset utilized for constructing the model was collected under various weather conditions, many of which the model cannot compensate for due to the absence of certain factors (temperature, humidity, etc.). To address this limitation, the dataset was divided into several groups characterized by similar weather conditions determined from pilot experience, yet with sufficient wind and spatial variations to enable effective modeling.

The modelling resulted in three versions of the model, one for each group of flights described in chapter 6. The flights used, classification into Case 2 or 3, and nominal wind is given at the end of this document.

The Model

The model employed a predominantly linear equation, incorporating variables measured within the aircraft itself, as well as data measurements obtained from the mast. Estimated Eddy Dissipation Rate over a 5-second interval (EDR5s) is approximated by the equation:

$$\widehat{EDR5}s = a \cdot D_{AV} + b \cdot D_{NS} + c \cdot H^2 + d \cdot H + e + f \cdot \bar{U} + g \cdot \bar{\theta} \qquad (1)$$

Here, D_{AV} represents the East-West distance (km, with east considered positive) from the center point (64.01, -22.11), while D_{NS} denotes the North-South distance (km, with north considered positive) from the same center point. H represents the altitude (m ASL) of the aircraft; the second order term is to allow for the mountain wave turbulence peak often observed at hill peak height, around 300m altitude in this case. Additionally, $\bar{U}$ signifies the 10-minute averaged wind speed (m/s) at a mast positioned approximately 30 meters above ground level (60 meters above sea level), and $\bar{\theta}$ represents the 10-minute averaged wind direction at the same mast location in degrees. Each measurement in the flight files was paired with mast data collected within 5 minutes of the flight reading.

The coefficients a through g in the model were determined by the least squares regression method.

The result from this analysis is presented by comparing directly the measured and predicted values in a scatter plot, as well as reporting model constants, R-squared and RMSE (Root Mean Square Error), where:

$$Rsquared = 1 - \frac{\sum_{i=1}^{N}(x_i - \hat{x}_i)^2}{\sum_{i=1}^{N}(x_i - \bar{x}_i)^2}$$

$$RMSE = \sqrt{\frac{\sum_{i=1}^{N}(x_i - \hat{x}_i)^2}{N}}$$

Results

EDR 5s Model and 20s

**Case1, all flight files. Case 2 flights 0-80 degrees. Case 3 flights 80-180 degrees**

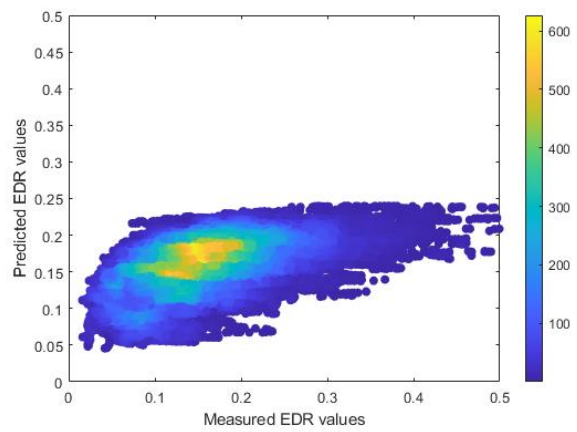| Coeff-icient	Case1 - EDR 5s	Case1 - EDR 20s	Case2 - EDR 5s	Case2 - EDR 20s	Case3 - EDR 5s	Case3 - EDR 20s
a (EW km)	0.002584	0.002717	0.002380	0.002481	0.003444	0.003623
b (NS km)	-0.005203	-0.005425	-0.005332	-0.005553	-0.005898	-0.006134
c (H m)^2	-2.47E-07	-2.58E-07	-1.55E-08	-2.95E-08	-4.77E-07	-4.85E-07
d (H m)	9.01E-05	9.80E-05	-1.36E-04	-1.26E-04	3.01E-04	3.07E-04
e (m$^{2/3}$/s)	0.113110	0.114130	0.186440	0.187630	0.092209	0.093592
f (U m/s)	0.002151	0.002365	0.002367	0.002593	0.005966	0.006243
g (θ deg.)	0.000294	0.000306	-0.000544	-0.000541	-0.000141	-0.000137
Rsquared	0.187	0.267	0.198	0.267	0.164	0.263
RMSE	0.071	0.058	0.067	0.057	0.071	0.054

Model comparison and data scatter

Below demonstrates the difference between the 3 models for one point in the area (7km, -7km,300m) for a wind speed of 12 m/s, and variable wind direction. Note Case 2 is only intended for 0-80 degrees and Case 3 only for 80-180 degrees.

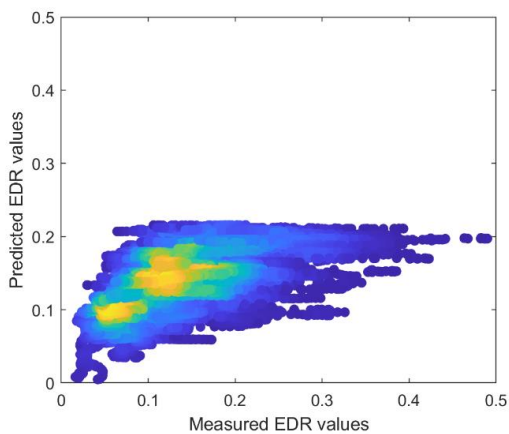EDR at 7km, -7km, 300m, 12m/s, variable degrees
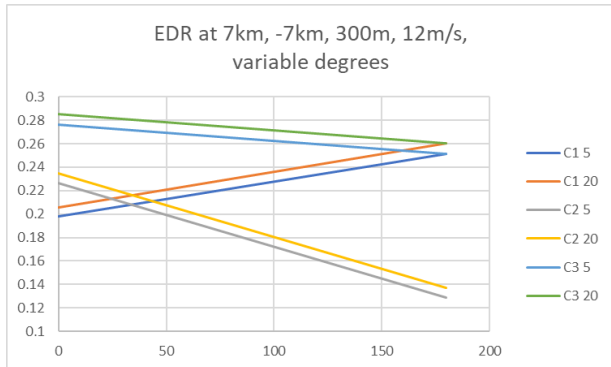
The data is very scattered, and the below graphs display the data pairs (measured - predicted) with color coding to indicate the frequency of each pair.
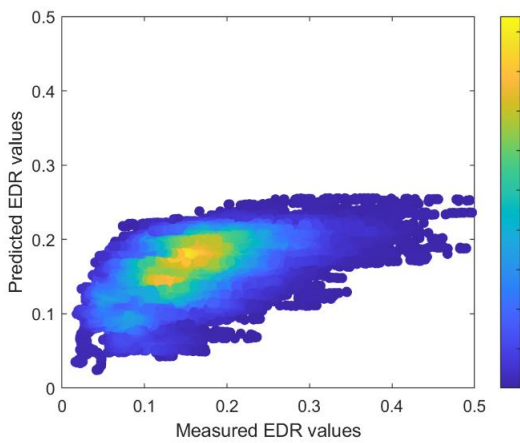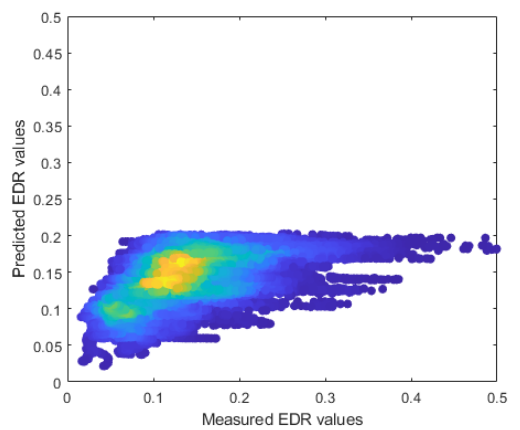

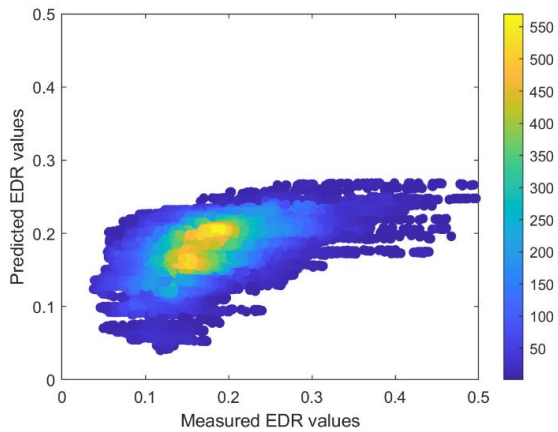Case 1, EDR 5s – measured vs predicted

Case 1, EDR 20s – measured vs predicted

Case 2, EDR 5s – measured vs predicted

Case 2, EDR 20s – measured vs predicted

Case 3, EDR 5s – measured vs predicted
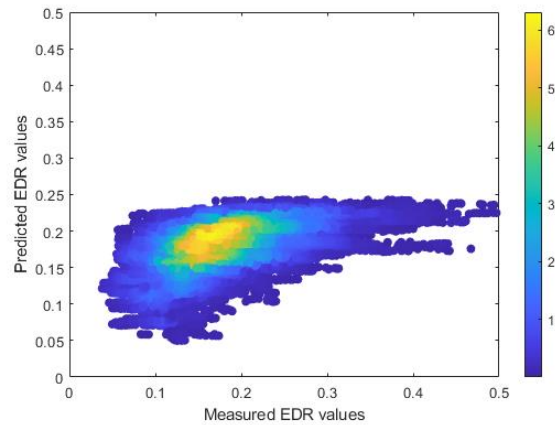
Case 3, EDR 20s – measured vs predicted

Comparison of models to real flights

The model coefficients for the five second and twenty second EDR are very similar, the 20s Model is slightly higher than the 5s model. Below are several graphs in each case that show flight measurements, and model predictions from both models. The 5s model is given in blue, the 20s model is given in red, and the flight data is given in green. It is clear from viewing the graphs that both models capture the same low-frequency dynamic. There are slight deviations, for example in the fourth graph in case 1, but they are minimal.

Case 1
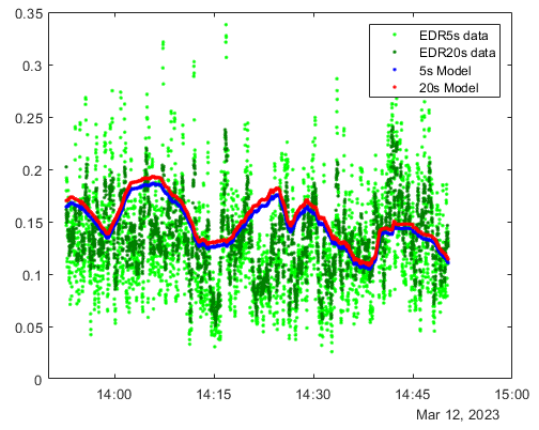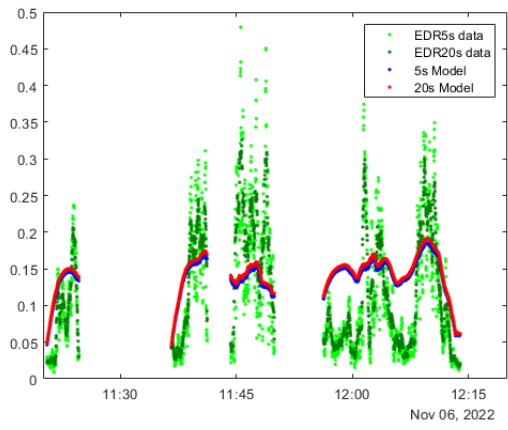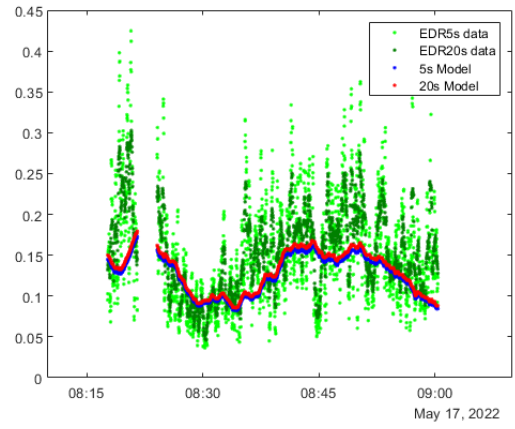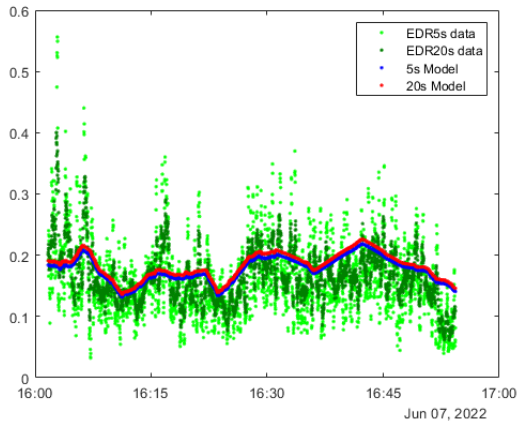
Case 2
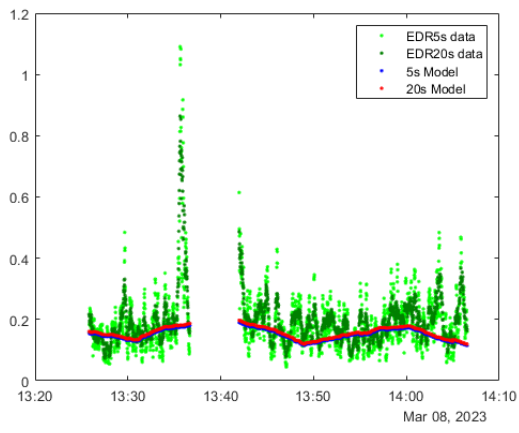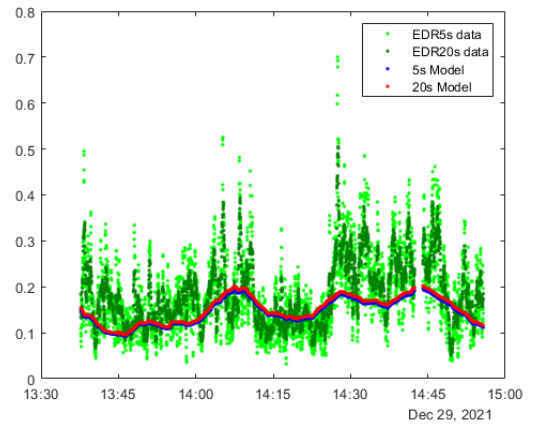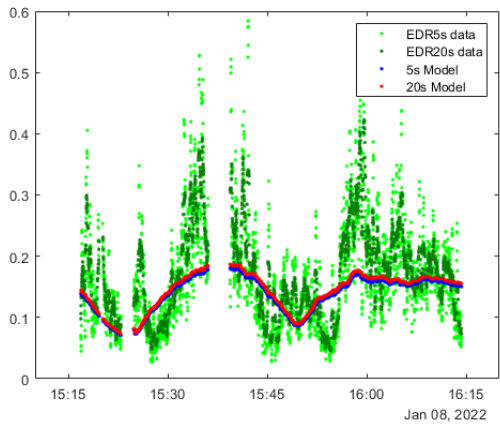
Case 3
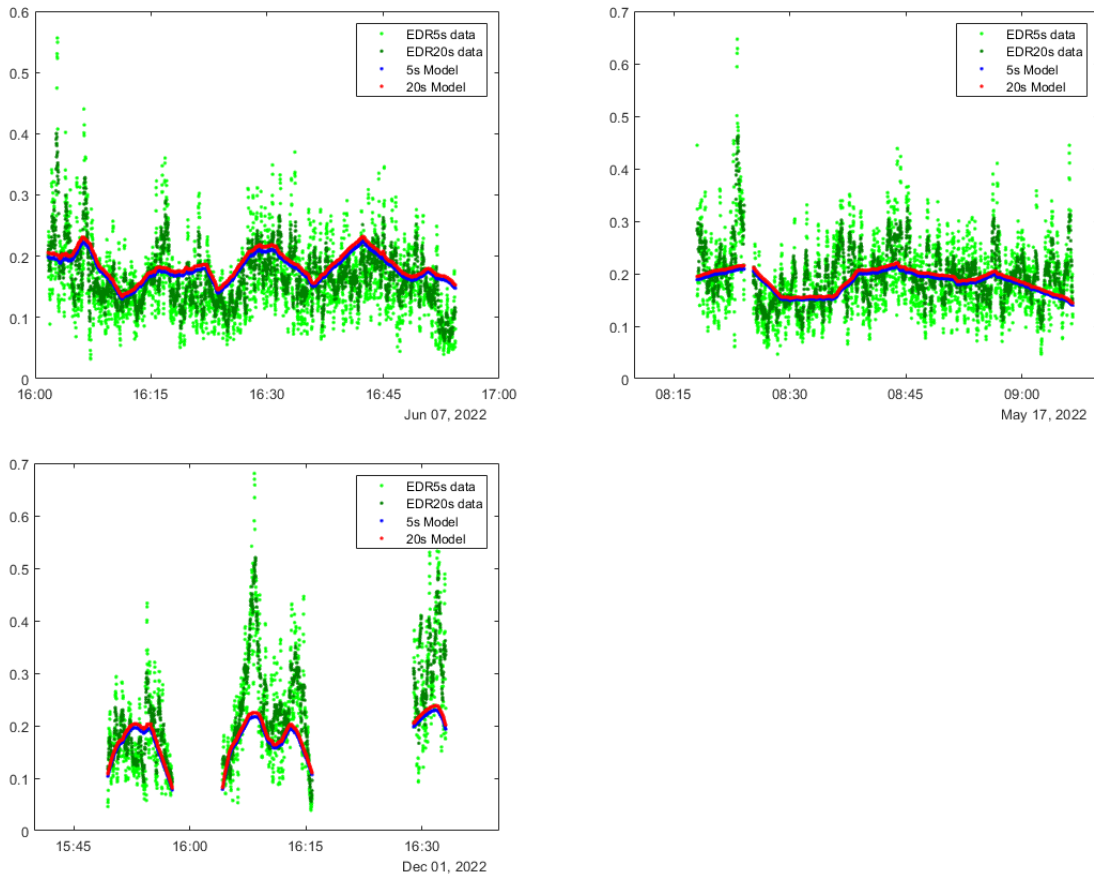
Correlation to EDR measured in the mast

EDR is estimated in the mast, so we could redo the above curvefits by exchanging mast EDR for the wind speed. We demonstrate this here, but for Case 3, 5s only. See also scattergraph of the measuerd – predicted data pairs.

Coefficient	Case3 – EDR 5s
a (EW km)	0.003900
b (NS km)	-0.006662
c (H m)^2	-4.51E-07
d (H m)	2.78E-04
e (m$^{2/3}$/s)	0.066304
f (edr_max)	0.539280
g (θ deg.)	-0.000542
Rsquared	0.199
RMSE	0.0703
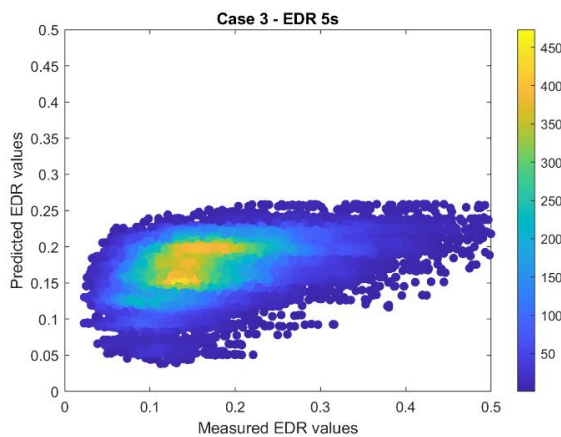
If we take the point (7km, -7km, 300m) as representative for highest value in the area of interest, then we can see that this correlation yields a lower value in the mast up to EDR of 0.25, but after this a lower

14

value appears at (7,-7,300) than at the mast. Observation of the data indicates that as windspeed (and EDR in mast) increases, the EDR in mast appears to be the highest average in the whole area of interest. The below graph displays all EDR data plotted against the same time frame EDR measured at the mast. Also plotted are red points representing the above correlation for the point (7,-7,300). In high wind, it is conceivable to use EDR max from 30 m mast to yield an upper limit of the highest EDR (average) in the area, when evaluating for which airplanes flying might be at a risk of meeting severe turbulence.
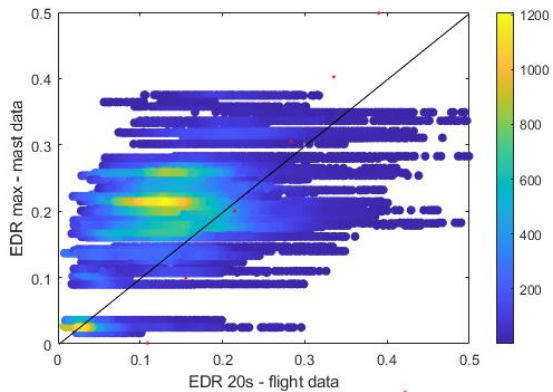
Flight date used in each case

File		Case	Nominal dir (deg)	U (m/s)
'2021_12_29_1'		2	21	7.5
'2021_12_29_3'		2	21	7.5
'2021_12_29_4'		2	21	7.5
'2021_12_22_1'		2	61	5.4
'2021_05_25_1'		3	130	9.9
'2021_08_23_1'		3	145	11.5
'2022_11_06_3'		2	61	5.8
'2022_12_01_4'		3	166	11
'2022_05_17_1'		3	87	7.2
'2022_05_17_3'		3	87	7.2
'2022_05_17_4'		3	87	7.2
'2022_05_16_2'		3	101	8.8
'2022_05_16_3'		3	101	8.8
'2022_05_16_4'		3	101	8.8
'2022_05_15_4'		3	149	8.8
'2022_06_07_1'		3	134	9.7
'2023_03_08_1'		2	63	12
'2023_03_12_4'		2	13	11.6
'2023_03_28_1'		2	63	8.3
'2022_05_02_3'		3	107	4.7

'2022_01_08_1'	2	45	8.2
'2022_01_08_3'	2	45	8.2
'2022_01_08_4'	2	45	8.2

Appendix C: How LIDAR vertical profiles were drawn for the data provided by Veðurstofan.

The Data

The LIDAR data was collected in two locations, one near the mast (64.01 N, - 22.1 E) spanning the dates from September 2022 to Januar 2023, and the other near the mountain range (63.97 N, -21.96 E) spanning January 2023 to May 2023. The LIDAR collects the standard deviation of wind speed, which can be converted to EDR by multiplying the values by 0.335. The data are time series given at 19 discreet vertical heights, specifically 100m to 1000m at 50m intervals. The LIDAR data has many empty values (77.8% missing near the mast, and 58.8% missing near the mounains), but values are generally available for most of the vertical heights if data is avaible at that particular time. In simple terms it means that there are many completely empty rows, and a couple of mostly full rows.

Data from the mast was paired with the LIDAR data. The mast collects wind speeds, wind direciton, and EDR at 2, 10, 20 and 30m heights. During this analysis, EDR was available until 10th of December 2022, after which no EDR values were availble from the mast. The mast data serves two purposes in this analysis, firstly it gives the low level EDR profile where data is availble. This is useful to compare to the LIDAR profile, and see the whole vertical profile from ground level to flight level. A seperate analysis pairs the LIDAR with the flight. Secondly, the data was used to filter for specific wind conditions, that is a wind speed minimum value and wind direction sector (0 – 45°, 45 – 90°, etc.).

The Processing

Each LIDAR data file (one for each location) is imported seperately and paired with the mast data. This is done by taking the time entries in the LIDAR data, and searching for data in the mast data files. The data was then filtered for wind speed minimums (8 m/s or 12 m/s) and the following wind sectors:

Sector 1	0 – 45°
Sector 2	45 – 90°
Sector 3	90 – 135°
Sector 4	136 – 210°
Sector 5	210 – 250°

Since LIDAR data was paired with mast data, they are both filtered at the same time. For each sector, the LIDAR data is averaged in each vertical height and empty values were skipped. Finally each average is multiplied by 0.335 to obtain EDR. The profiles are then plotted on the same figure with the number of data points (N) average wind speed (AvgSpd) and average wind direction (AvgDir) reported for sector in

the legend. The figures resulting from this analysis are shown below. There are two figure for each location, for 8 m/s wind and over, and another for 12m/s and over. The higher speed limit loses a significant amount of data in some sectors.

Results and Dicsussion

LIDAR vertical EDR profile near the mast is shown in Figures 1-2.
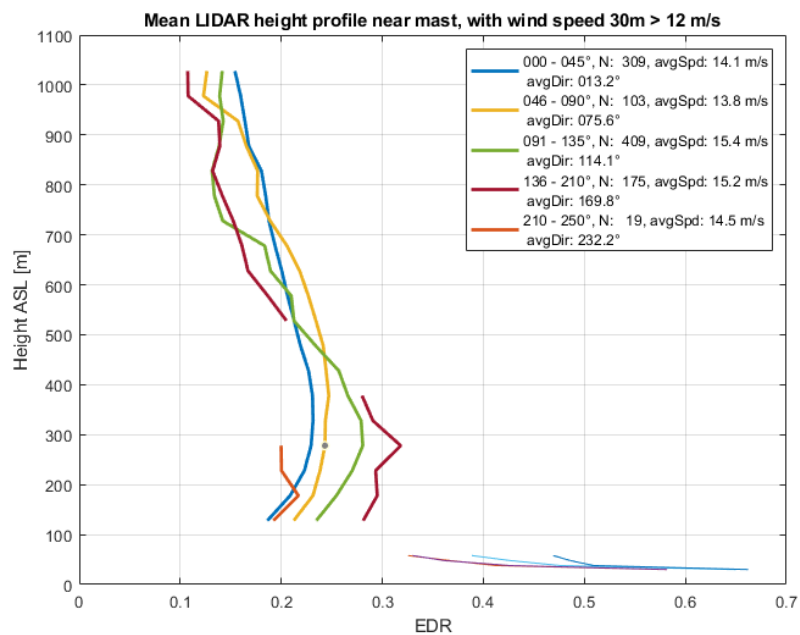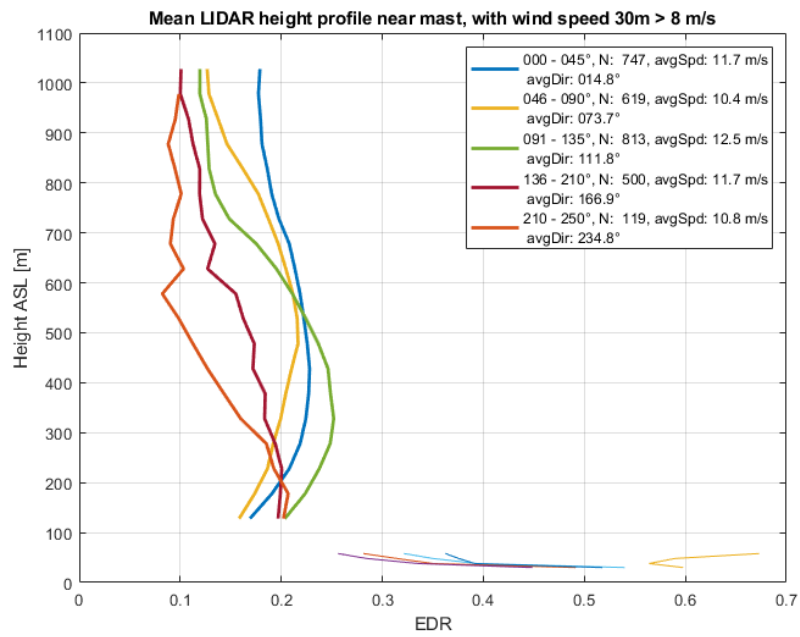
Figures 1-2: Vertical EDR profiles near mast for two wind speed minimums.

The EDR vertical profiles in general seem to decline with height, however the wind sectors of 0 – 135° tell a different tale. They seem to initially increase with height, reach a maximum and start to decline. The maximum average EDR for the 8m/s limit figure is in at ~350m ASL, in the 90 – 135° sector. Increasing the wind speed limit drops a significant amount of data points in the wind sectors of 136 – 250°, and the maximum EDR value is now in the 135-210° at ~280m ASL. It should also be noted that the EDR LIDAR profile in the sector 210 – 250° is inline with the others, however the mast profile in that particular sector was much higher (see Figure 5 and discussion).

LIDAR vertical EDR profile near the mountains is shown in the two figure below.
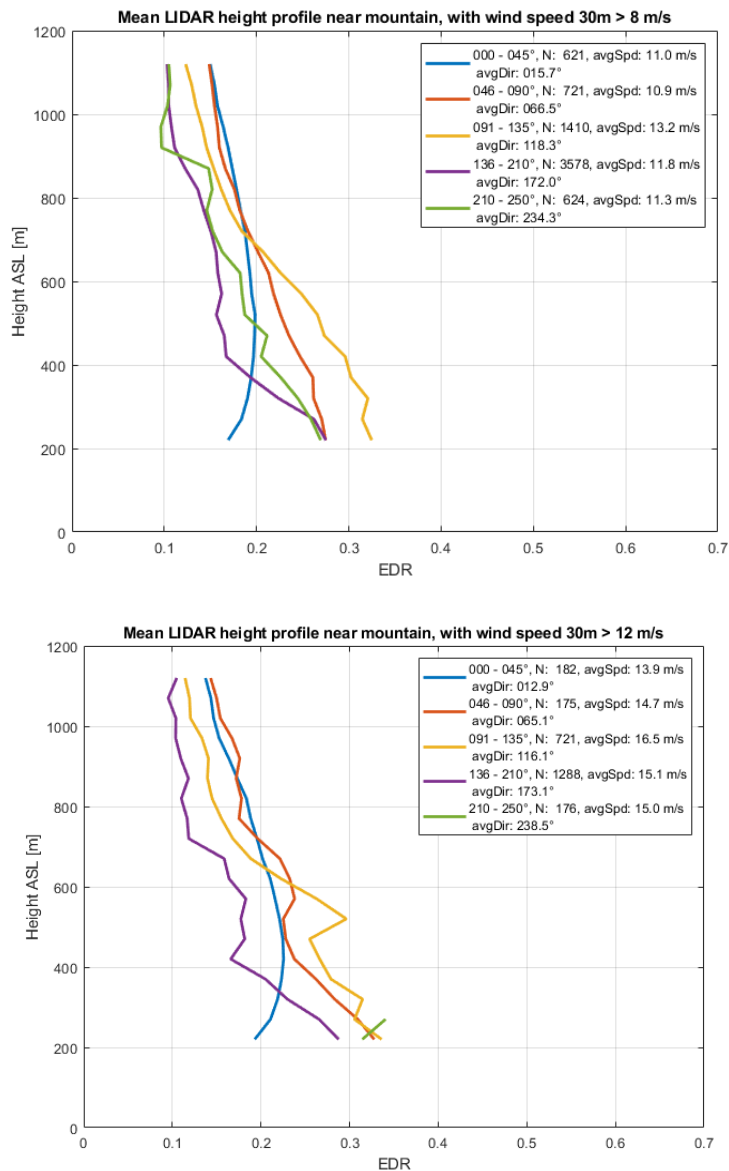
Figure 3- 1: Vertical EDR profiles near mountains for two wind speed minimums

In general, the EDR profiles seem to decline with height and the distinct profiles mentioned near the mast are not present or clearly visible near the mountains. It is likely the effects of the mountains have not developed yet for the same phenomena to occur. The highest average EDR is again measured in the 90 – 135° sector at 8m/s minimum, at the lowest recorded EDR ASL.

Figure 5 shows the LIDAR vertical profile near the mast, and marks the 210 – 250° sector in black, while the others are blue and red. Even though the LIDAR profile gives the smallest value of EDR at most heights, the mast measured significantly higher values than any other wind sector. It also has the maximum EDR at 30m height, unlike every other mast profile, where the EDR decline rapidly with height as the low-level turbulence dissipates. There was speculation whether the mast frame interferes with the measuring sensors given the proximity of the sensors to the frame, and Figure 5 seems to substantiate that speculation.
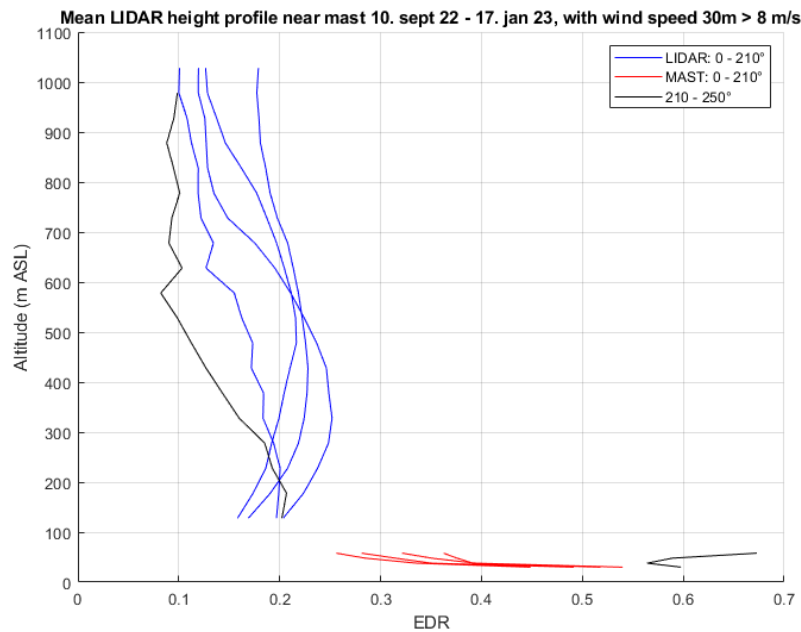
Figure 5: Vertical EDR profile near the mast for 8m/s. The 210 - 250° is shown in black, both for LIDAR and mast.

Appendix D: Forecast comparison

1. Introduction

This document describes evaluation of potential utility of meteorological forecasts for the area defined in [Section x in this document] for the purposes of replacing weather measurements collected by a ground mast in the area for low level winds and in-flight measurements for high-altitude winds.

The meteorological forecasts for the area were provided by Belgingur ltd. (Belgingur). The forecasts were compared with measurements collected from a mast located in are (Straumsvík) and in-flight measurements collected by two types of airplanes (light and medium) for the same area. This comparison was then used to evaluate the potential of the Belgingur meteorological forecasts to be used to forecast EDR (please refer to Section [●] in the main text for definition of EDR) in and around the airport.

This is useful to cover gaps in the measurement program that were hard to fill.

The comparison in this study started by comparing the forecasts with the measurements obtained from the mast. The factors that were evaluated were wind speed, wind direction and EDR measurements. The mast measurement was considered more reliable than the in-flight measurements, given that the mast is fixed in place, and it measures the factors at the same time-average windows as the forecast predicts for.

The aim was to determine if the meteorological forecast is an accurate description of local weather conditions, that have considerable effect on turbulence phenomena encountered in flight. This would further give credibility using meteorological forecast to predict in-flight factors.

The analysis in this document lacks the vertical profile of weather conditions up to the altitudes flown needed to which are needed to evaluate with more precision the accuracy of the ground-based measurements.

At the outset of this comparison the intention was to obtain data from a LIDAR that measured EDR at altitudes of 100m to 1000m. Data containing the vertical profile of weather conditions up to the altitude however were never made available to analyze.

The study further investigated the performance of the Belgingur meteorological forecasts for the area by comparing them to in-flight measurements collected from flight routes over the same area. The factor evaluated was EDR, the airplanes did not collect windspeed nor direction in-flight.

This document describes the measurement data, how the Belgingur meteorological forecasts are generated and processed, the statistical properties used to evaluate the accuracy of the forecasts. Finally, findings are reported in this document with a variety of graphs to evaluate the accuracy.

2. Method

2.1 Mast Data

Wind speed, wind direction and EDR measurements were obtained from a mast (64.009322,-22.140447) close to the airport site (N 64.01, E -22.11) managed by Veðurstofan. The data collected are 10-minute averages (from January 1st, 2021, to December 31st, 2022) of the variables measured at 2m, 10m, 20m, 30m height above ground level. Given the focus on high altitudes, only the 30m height was used to avoid the interference of terrain induced turbulence, which has minimal relevance to the overall report.

Important fact to note is the interference of the steel structure to the measuring probes in wind directions of 210 – 250°. A picture is given below. Close proximity of the sensors to the mast has been shown to interfere with measurements, in particular with EDR estimates. This is explained by the fact that the steel frame generates small scale turbulence.

Figure 1: Photograph of mast location. Taken from Google Earth Pro.

---- Mynd af mastri ----

2.2 Flight data

For detailed descripiton of in-flight measurement methods and weather condition program, refer to section [●] in this document .

The measurements that were used in this comparison were reported in 1s averaged intervals. The variables reported were latitude, longitude, altitude, EDR5s, and several others that are not relevant in the comparison.

2.3 Belgingur forecast data

Given the relatively small size of the area of interest for weather forecasting and the desire for better accuracy and resolution, the Belgingur meteorological forecast was generated using a grid size of 600 meters (instead of the normal 3km).

It should be noted that Belgingur meteorological forecast interpolates values when the aircraft location did not align with the forecasts grid.

Accessing the forecast data involved utilizing an "Application Programming Interface" (API). Users were required to specify various parameters, including geographical location (latitude and longitude), altitude, either above sea level (ASL) or above ground level (AGL), variable (wind speed, direction, or EDR), and the specific forecast job (Forecast Job). A Forecast Job refers to a computational process that predicts weather conditions over a specific time period (generally specified by the starting time of the forecast). Several meteorological variables, such as wind speed, wind direction, and EDR were simulated for the time period at time intervals of 10 minutes. After computing a prediction, the Belgingur forecast receives measurement data from local sensors in Iceland, as well as grand scale weather variables from [●] to adjust the forecast. This is done every 2 hours before the 8th of August 2022, and every 3 hours after.

When evaluating how a Forecasting Job is to be used, the researchers discovered two things. Firstly, in the initial first two to three hours over the Forecasting Job, the model was adjusting to the correcting sensor and grand scale data mentioned before. Secondly, the forecasts grew more inaccurate as time went on. For this reason, it was decided to limit the time period of each Forecasting Job to 2 hours in dates before 8th of August 2022, or 3 hours in dates after 8th of August 2022. It was further decided to omit the first 2-3 hours of each Forecasting Job for the purposes of obtaining more accurate forecasts. In the case of comparisons that lasted longer than 2-3 hours, or spanned multiple Forecasting Jobs, sequential jobs were spliced together to ensure that no transient or period over 3 hours was used. Figure 2 shows a graphical representation of how this was carried out.
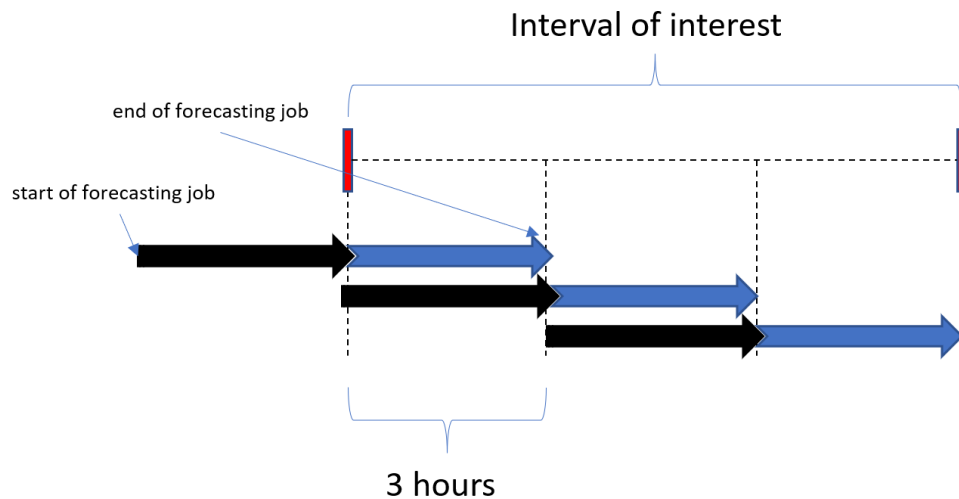

Figure 2: Splicing of forecasting jobs. Blue arrows are the portions of forecasting jobs that are used in the comparison. Each pair of black and blue arrows represents a forecast job.

2.4 Statistical coefficients

The statistical coefficients reported in the results are as follows:

- Coefficient of determination (R squared)
- Root Mean Square Error (RMSE)
- Bias

R squared is a coefficient from spanning the range 0 to 1 that represents how well the model is performing. It can be interpreted as the proportion of the variation in the measured values that can be explained by the forecasted values. The following equation is how the coefficient was determined:

$$Rsquared = 1 - \frac{\sum_{i=1}^{N}(x_i - \hat{x}_i)^2}{\sum_{i=1}^{N}(x_i - \bar{x}_i)^2}$$

RMSE represents the error of the forecast model. It has the same units as the variable it is quantified from.

$$RMSE = \sqrt{\frac{\sum_{i=1}^{N}(x_i - \hat{x}_i)^2}{N}}$$

The final coefficient, Bias, is useful to determine whether the forecast is underestimating or overestimating the variables of interest. It was determined by the equation:

$$Bias = \frac{1}{N}\sum_{i=1}^{N}(x_i - \hat{x}_i)$$

where x is either windspeed or EDR, $\hat{x}$ is the forecast prediction of the variable, X is a collection of measured values of x, and $\hat{X}$ is the collection of predicted values $\hat{x}$.

To compare the directional component of the forecast, a method detailed in [x] (https://www.researchgate.net/publication/358584884_Wind_and_Gust_Forecasts_Assessment_of_Weather_Research_and_Forecast_WRF_Model_in_Cordoba_Argentina) was used although a bracket was added in the secondary condition in the fork, since the original did not add up. The variable defined there is $\Delta\theta$ and is defined by the equation:

$$\Delta\theta = \begin{cases} \theta_{for} - \theta_{obs}, & \text{if } |\theta_{for} - \theta_{obs}| < 180° \\ (\theta_{for} - \theta_{obs})(1 - \frac{360}{|\theta_{for} - \theta_{obs}|}), & \text{if } |\theta_{for} - \theta_{obs}| < 180° \end{cases}$$

$\Delta\theta$ represents the forecast deviation of the forecast form the observed wind direction. This method is useful since it deals with the nonlinearity between $0 - 360°$.

3. Results

The comparison of forecasted windspeed and EDR to measured values at 30m height above ground was carried out. The analysis was reported in wind sectors, each interval spanning 45° from 0° to 360°. The dataset was split into wind sectors by using the measured wind direction of each pair of forecast and measured value. Therefore there are 8 graphs for both windspeed and EDR comparisons, each graph reporting the Rsquared, the slope term in a linear fit (a), and the intercept in a linear fit (b). To compare the wind direction, the method specified in 2.4 was used where the direction deviation is specified as a function of windspeed.

3.1 Wind Speed

The results from the comparison can be seen in Figure [●]. The Rsquared coefficient is similar across all wind sectors, spanning 0.45 to 0.72. However there seems to be higher correlation between the forecast and measured values as the wind direction surpasses 180°. Another factor to consider is the slope of the linear fit. In wind directions of 0 – 180° the slope of the line spans the range of 0.68 – 0.75, which suggests that the forecast underestimates the windspeed in those directions. As the wind direction goes over the 180° the slope term spans the range 0.87 – 0.93. This indicates that the forecast is more accurate in those sectors and underestimates less. The intercept term remains similar across every wind sector, although it reaches the lowest value of 0.35 in 315-360°.
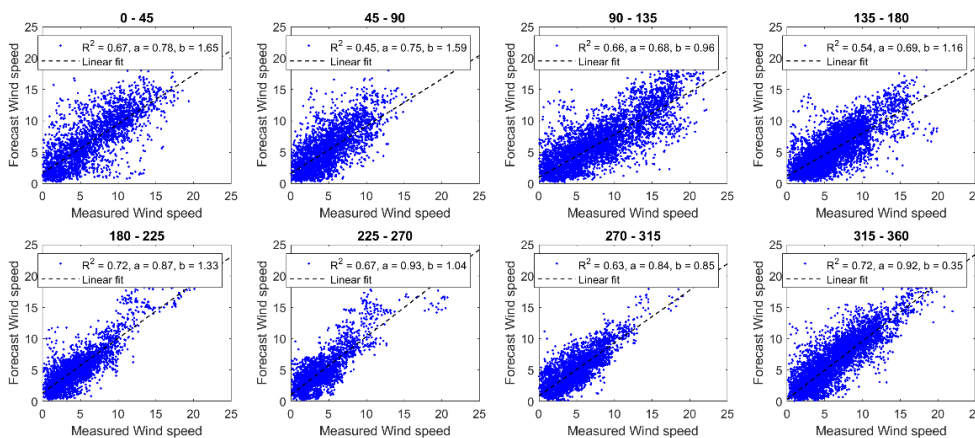

Figure ##: Comparison of forecasted wind speed to mast wind speed.

3.2 Wind Direction

Figure [●] shows the deviation of wind direction as a function of wind speed. The deviation seems to be significant at lower wind speed than 5 m/s, with scatter points covering the entirety of the allowed range. This is to be expected, at low wind speeds the deviations in sensor measurements are much harder to predict and are more subject to small scale local effects rather than large predicable weather patterns.

However, as the windspeed goes over 5 m/s it is clear that the wind direction becomes more accurate. The forecast has a slight positive bias of 5.6°, indicating that the forecast slightly overestimates (counterclockwise) the wind direction. Given that the greater study is focused on weather conditions with significant wind speeds (at least above 5 m/s) the results are good.
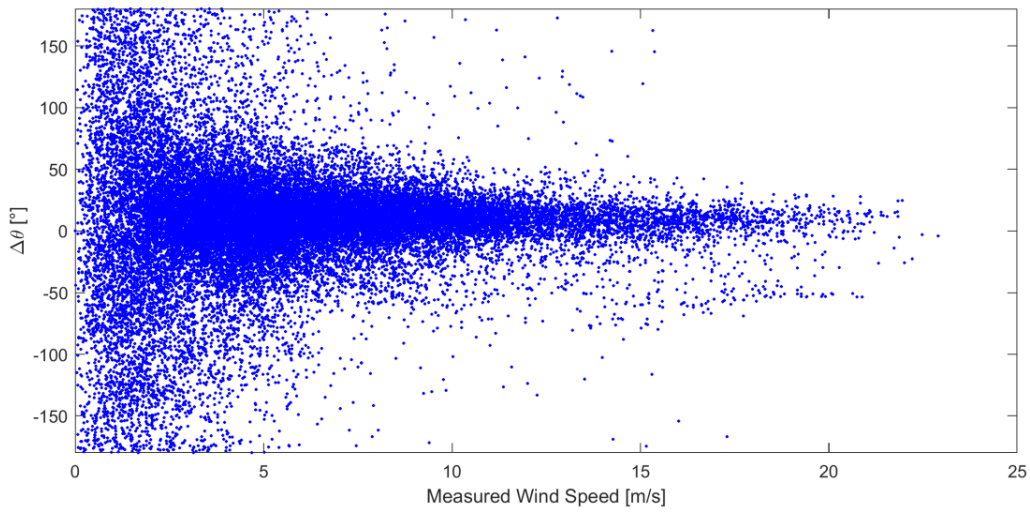
Figure [●]: Deviation between forecast and measured wind direction as a function of wind speed.

3.3 EDR

The results from the comparison can be seen in Figure [●]. Statistical coefficients are reported in the same fashion as for wind speed. The Rsquared coefficients span a range of 0.47 to 0.72, with linear slopes ranging from 0.32 to 0.77. The aforementioned mast interference is clearly visible in the 180 – 270 degree range. Once again the sector of 315 – 360 is the most accurate, with among the highest Rsquared and a slope of 0.77 with a low intercept. Across the board the forecast seems to underestimate the measured EDRs although there is significant scattering along the linear fit line.
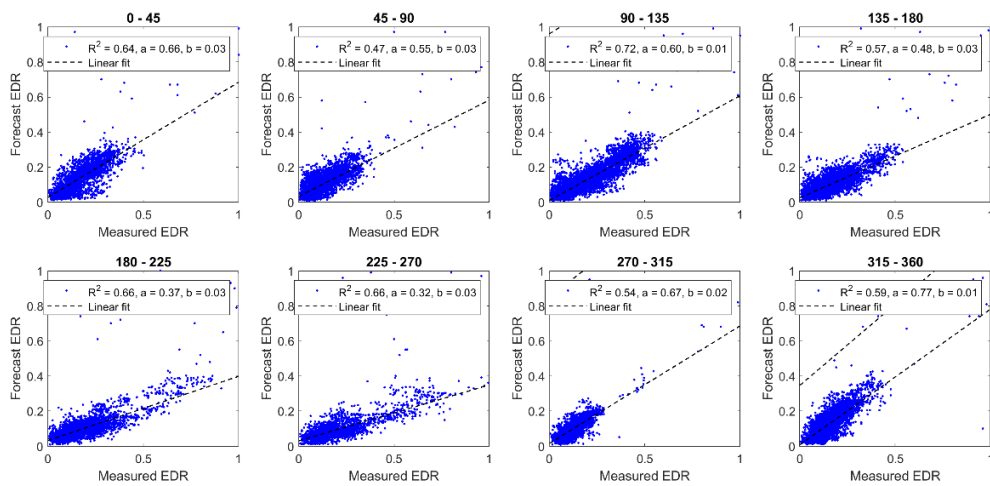

Figure [●]: Comparison of forecasted EDR to measured EDR.

3.4 Case studies of wind days

26

To gain a better understanding of how the forecast compares with the measured data, the values were compared on a 24-hour basis for a select number of days. Most relevant to the overall study were days where windspeed exceeded 15 m/s for a significant amount of time. Accurately predicting high EDRs ahead of time would be most useful for these cases. The case studies compare in Figures [●] the same values as the overall comparison, namely windspeed, wind direction and EDR. Each figure generated has the time on x axis from midnight of the starting to midnight of the next day. The figure has blue as values from the forecast and red as values from the mast. The emphasis was to analyze how accurately the forecast can place the time event of the turbulence, as well as analyze how accurately it predicts wind speed and wind direction in time.

061800061900

062300062400

112200112300
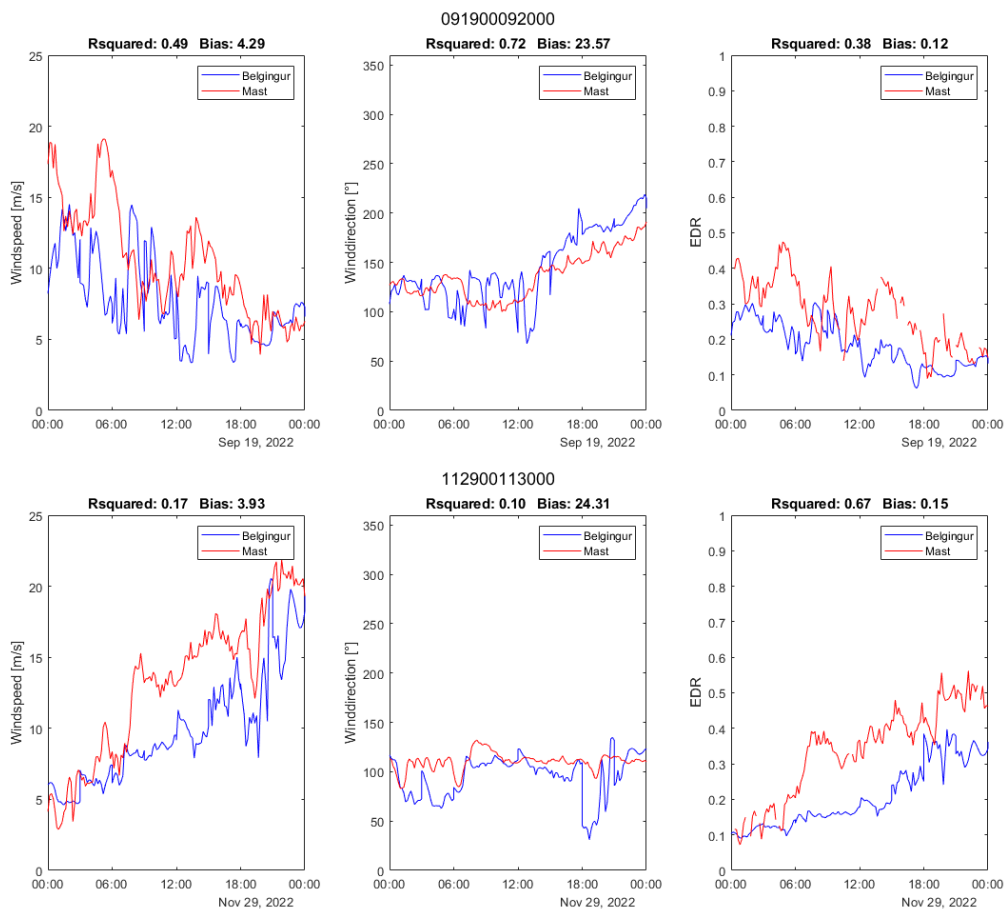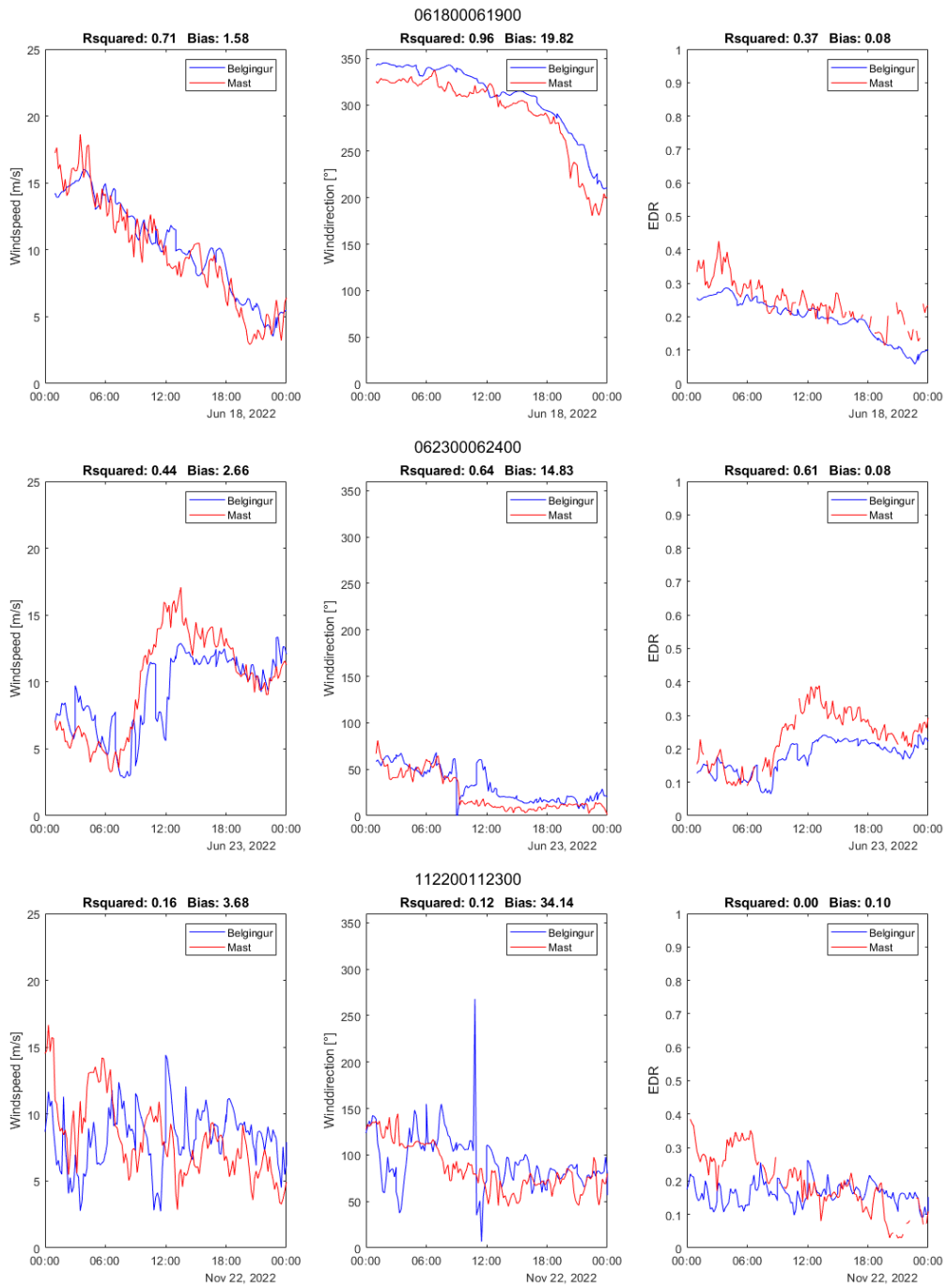
Overall, it is apparent that the forecast captures the dynamics of the atmosphere accurately. The forecast and measured trends follow along for the most part in wind speed and direction, although there are cases where the forecast predicts the opposite of what happens, for example on the 14th of November 2022 it predicts periodic oscillations in windspeed while the measured is a strong wind speed of over 15m/s.

When it comes to EDR the dynamics are captured well, with a bias of around 0.1 with Rsquared generally around 0.6 - 0.7. The figure above show why the inconsistent nature of the forecast makes it hard to rely on for individual cases of turbulence forecasting, since the forecast sometimes very accurately predicts the turbulence, while other cases it severely underestimates the turbulence.

3.5 Flight comparison

A number of flight tracks were compared directly with the forecast. The forecast was read at each coordinate reported in the flight data. The conditions present at 10m height at the mast is also reported. They were:

1. D8-200 – 1st of December 2022 (2022_12_01_4)
    a. 9 – 12 m/s, 160 – 175°
2. D8-200 – 6th of November 2022 (2022_11_06_3)
    a. 3 – 5 m/s, 41 – 74°
3. Savannah – 16th of May 2022 (2022_05_16_3)
    a. 7 – 8 m/s, 83 – 105°
4. Savannah – 17th of May 2022 (2022_05_17_3)
    a. 4 – 7 m/s, 65 – 90°
5. Savannah – 27th of May 2022 (2022_05_27_3)
    a. 3 – 4 m/s, 315 – 330°
6. Savannah – 7th of June 2022 (2022_06_07_1)
    a. 8 – 9 m/s, 135 – 140°

12 Figures are shown below in pairs of two, see Figure [●]. The date of the flight days is listed in each figure's title. The left most figures show time series comparison of flight data to forecasted data. The right most figures show a scatter graph of forecasted values as a function of measured values. The 1:1 dashed line is also shown in the right most figures. The right most graphs report the slope a, and intercept b, of a linear fit through the dataset, and the Rsquared coefficient.S
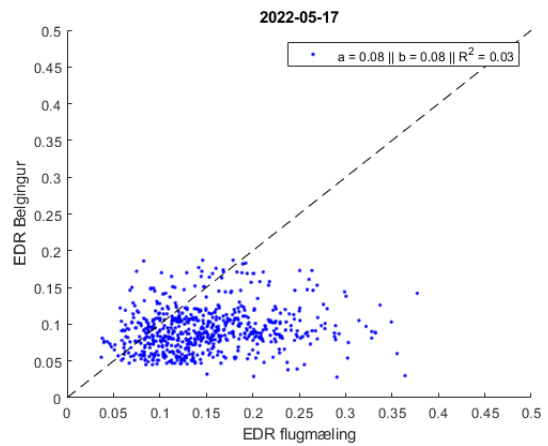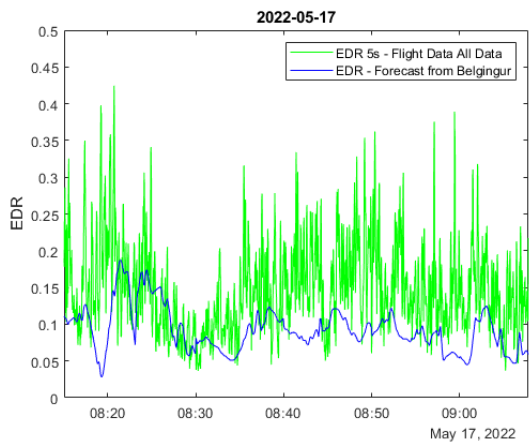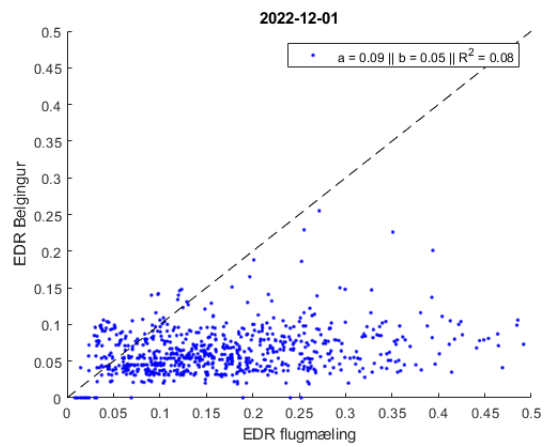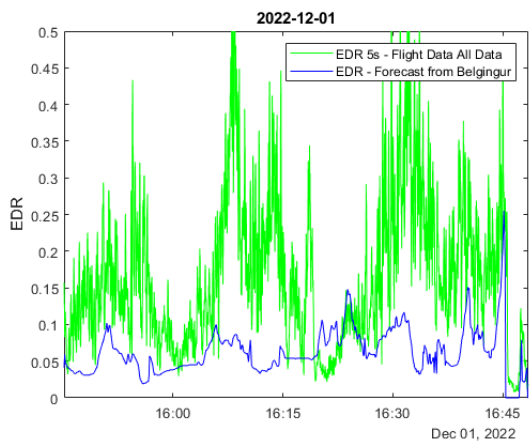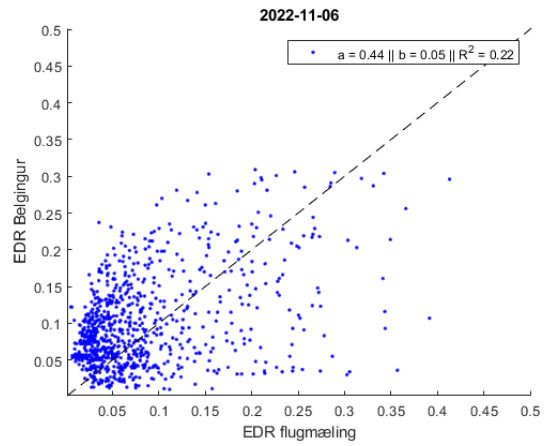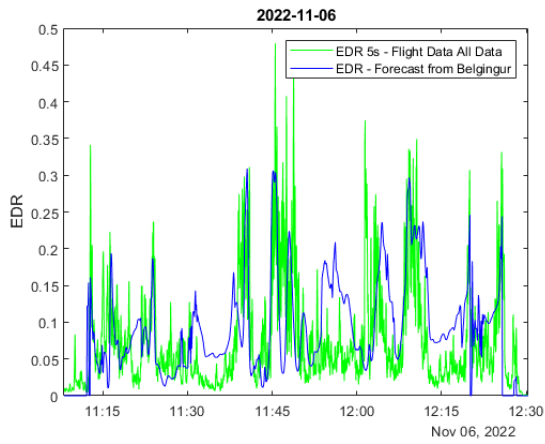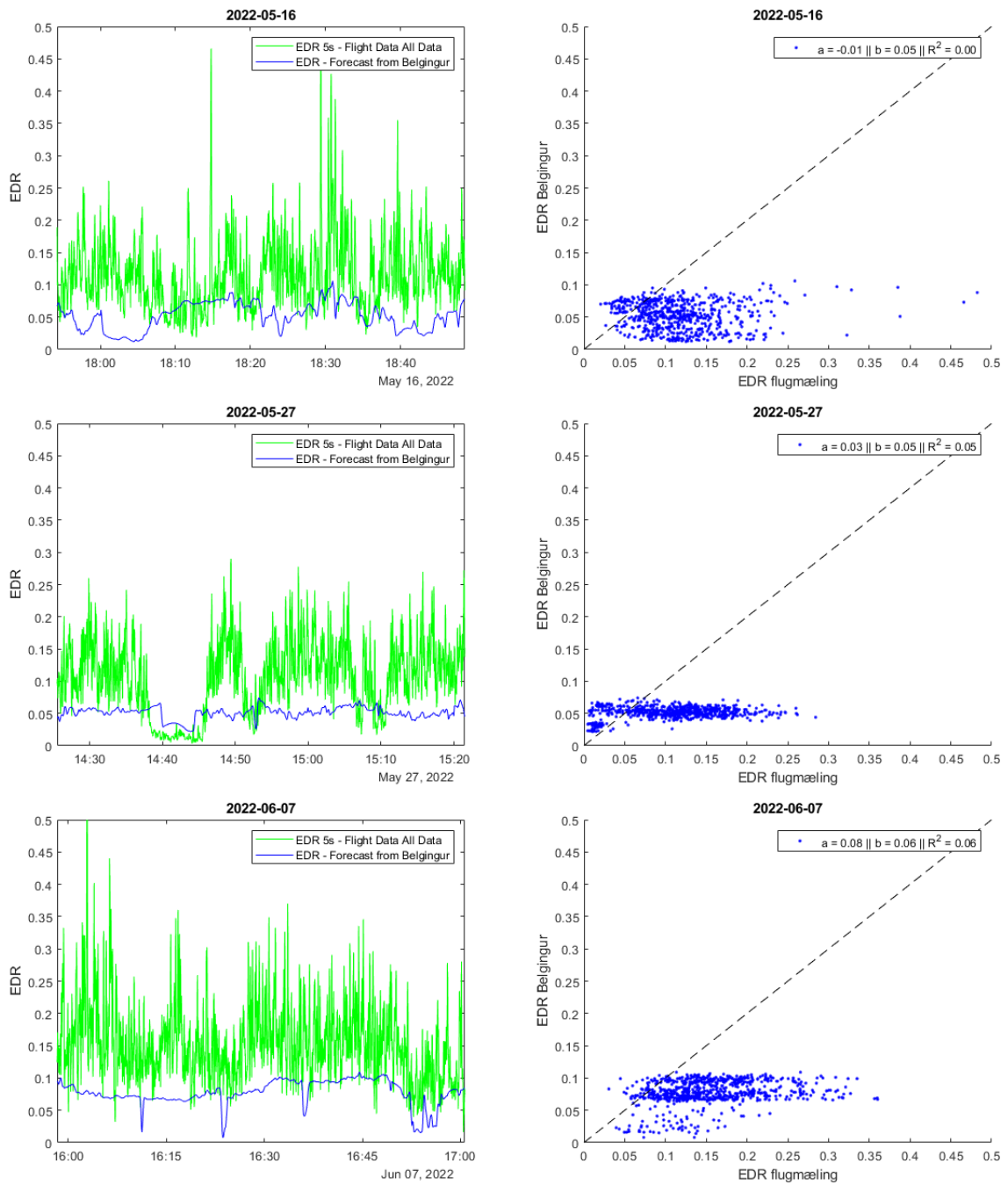
Figure [●]: EDR timeseries over the course of the flight. Red is flight data collected, and the blue is a simulated flight path through the forecasted EDR field.

Figures [●], [●], and [●] show inconsistent results. In some cases, for example 6th of November 2022, the forecast seems to fluctuate and match some of the peaks observable in the flight track. In other cases, forecasts predict peaks where measurements generated none.

In general, the forecast predicts a low value, generally well under the observed average of the flight data, and has low fluctuation in EDR value. The slopes of the linear fits range from -0.01 to 0.44, with coefficients of determination from 0 to 0.22, suggesting a low model fit.

4. Conclusion

In conclusion, this study aimed to evaluate the accuracy of the Belgingur weather forecasts by comparing them to measurements obtained from a mast in Straumsvík and in-flight routes of light and medium airplanes. The comparison with the mast measurements focused on wind speed, wind direction, and EDR measurements. The performance of the Belgingur forecasts was further assessed by comparing them to in-flight EDR measurements.

Belgingur meteorological weather forecast accurately predicts the dynamics of wind speed, wind direction and EDR in ground measurements, although there are cases where it predicts opposite trends. There are indications that the forecast in some instances underestimates both wind speed and severely underestimates EDR values.

When compared with in-flight measurements the forecast does not produce the same variation measured but seems to have the general underlying dynamics in the majority of cases.

112100112200

111700111800

111400111500

083100090100

Rsquared: 0.00   Bias: 1.90

Rsquared: 0.76   Bias: 26.21

Rsquared: 0.70   Bias: 0.13

082900083000

Rsquared: 0.36   Bias: 3.49

Rsquared: 0.53   Bias: 9.78

Rsquared: 0.67   Bias: 0.13
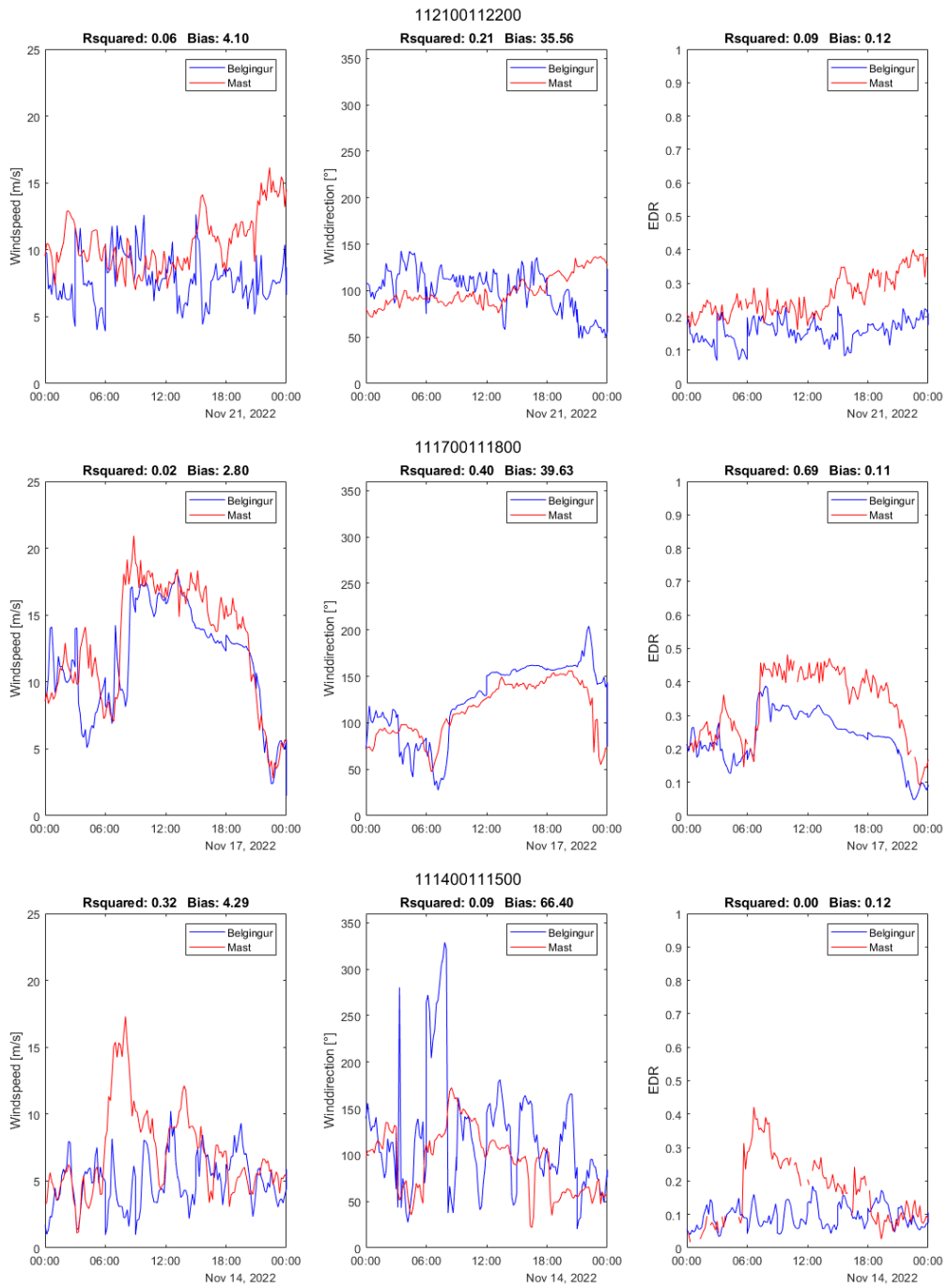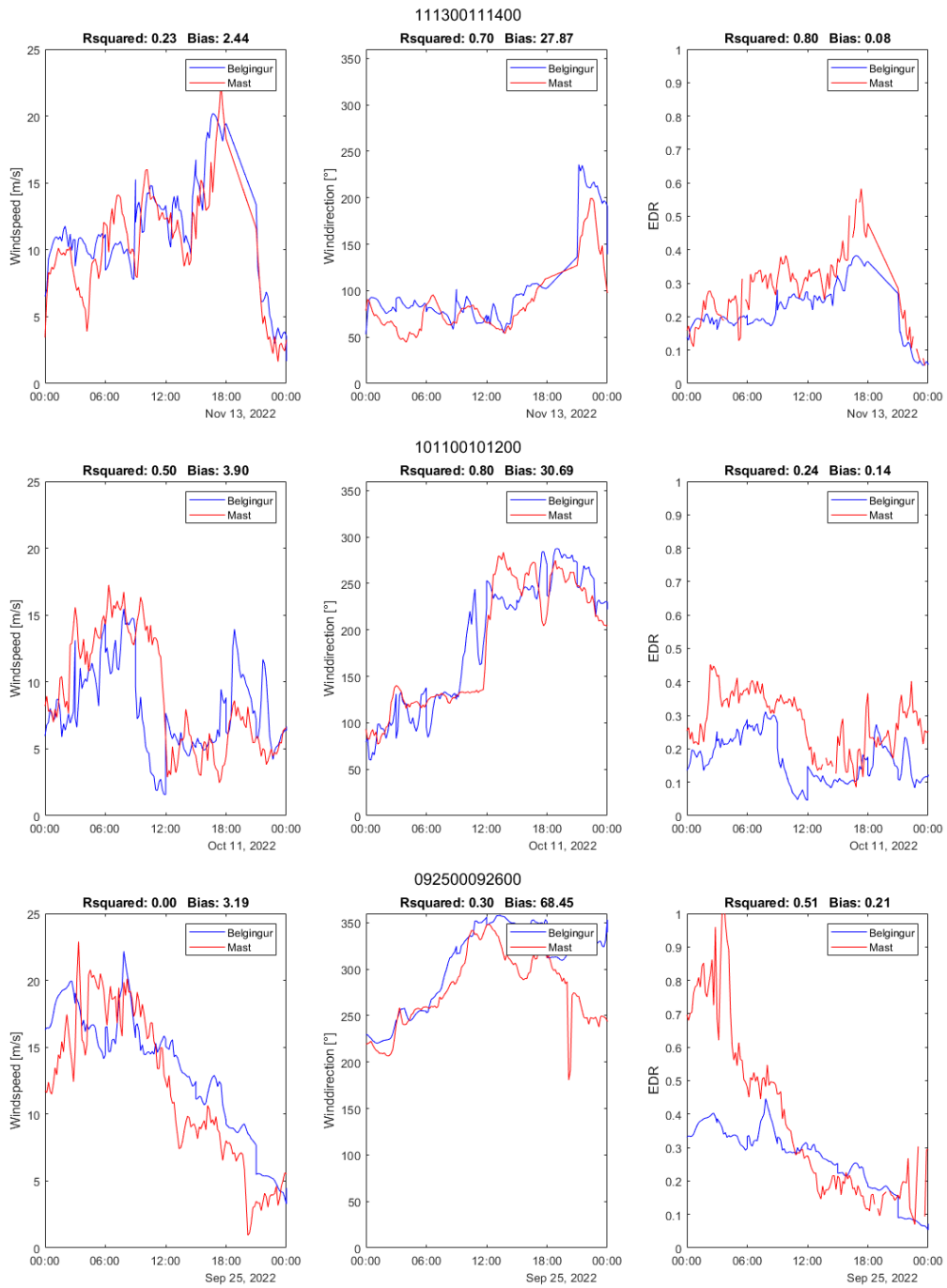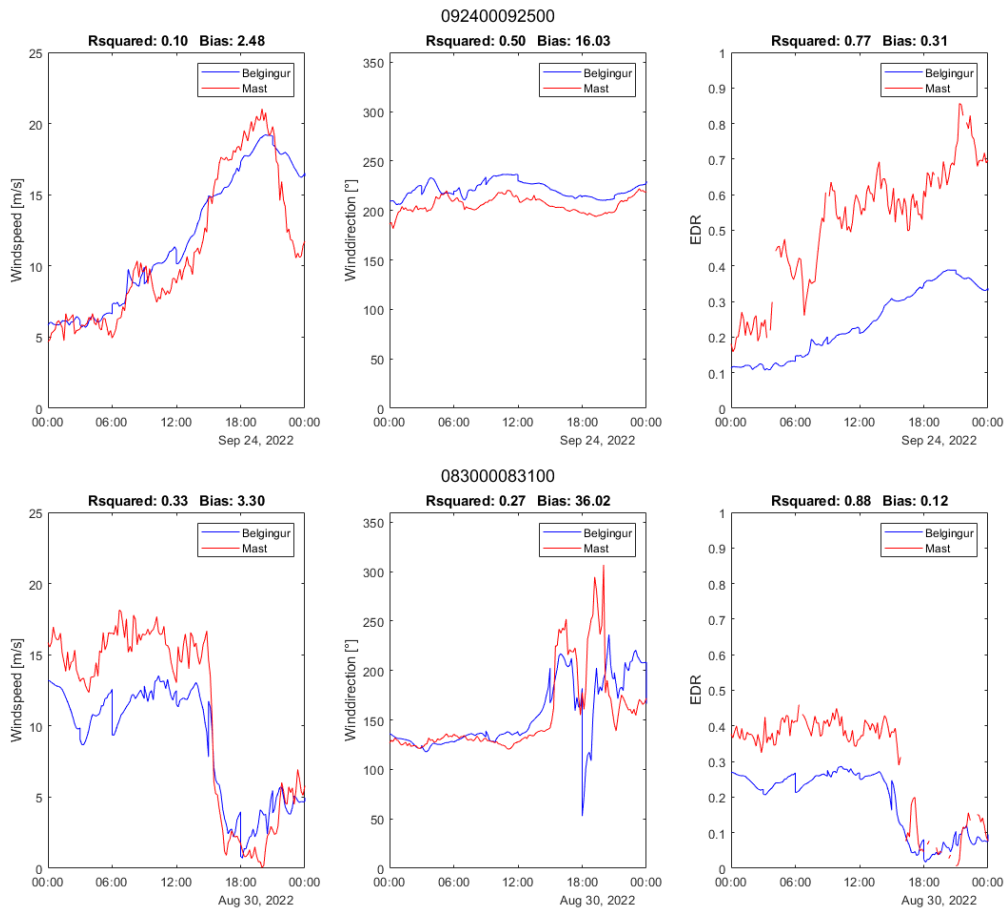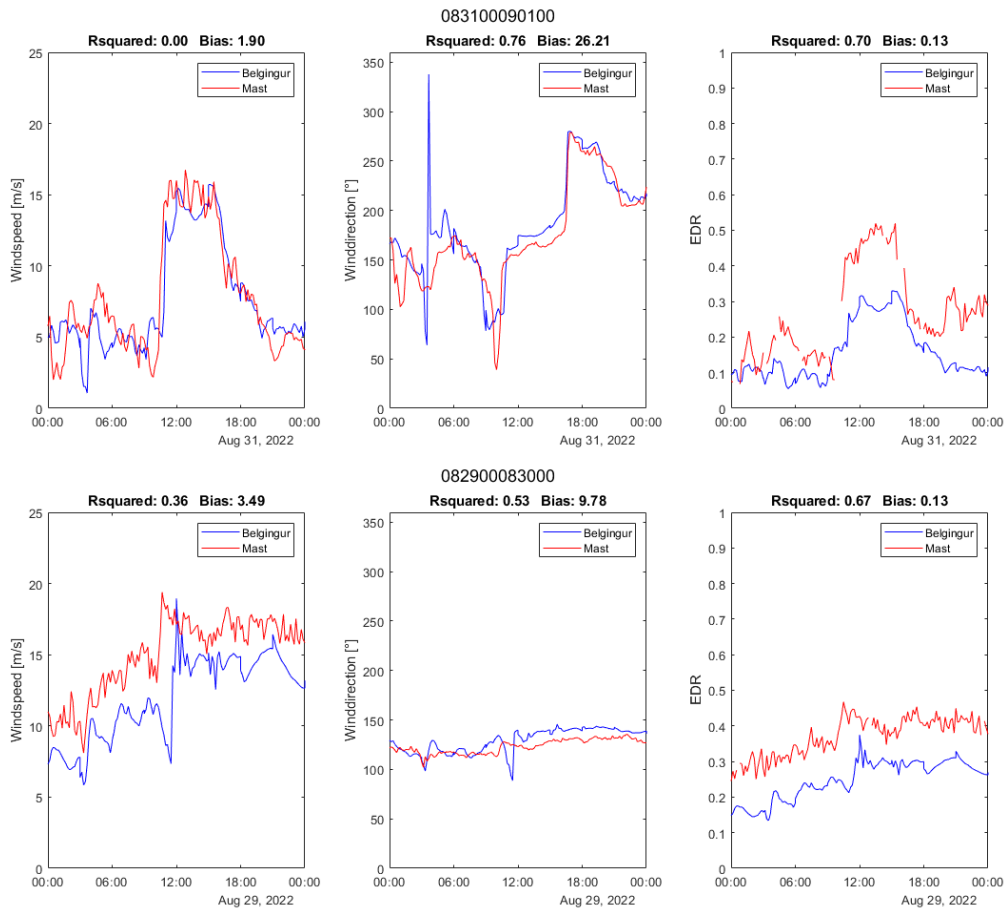
Appendix E: Groups – Similar Conditions in Hvassahraun.

After careful examination of the flight data it was concluded that we have 3 flow regimes; low wind, wind from directions 20-80 degrees (i.e. wind not fully crossing the hills SE of the area of interest) and wind from 80-180 degrees crossing the hills. Data was further analyzed in the above groups as is displayed below. Analysis included also curve fit of EDR-20-sek. These are initially correlated with mast wind speed and direction, but only with one nominal wind and direction value per track. We also do this analysis with mast values every 10 minutes of flight (presented in Appendix B; Correlation Model). The plots below stem from the data in Appendix B.

Overall curvefits (1: all wind directions, 2: 20-80 degrees, 3: 80-180 degrees, 4: no wind (convection))
1) filenames =
['2021_12_29_1','2021_12_29_3','2021_12_29_4','2021_12_22_1','2021_05_25_1','2021_08_23_1', '2022_11_06_3','2022_12_01_4','2022_05_17_1','2022_05_17_3','2022_05_17_4', '2022_05_16_2', '2022_05_16_3','2022_05_16_4','2022_05_15_4', '2022_06_07_1', '2023_03_08_1','2023_03_12_4', '2023_03_28_1','2022_05_02_3', '2022_01_08_1','2022_01_08_3','2022_01_08_4']

2) filenames =
['2022_11_06_3','2023_03_28_1','2023_03_08_1','2021_12_22_1','2021_12_29_1','2021_12_29_3', '2021_12_29_4', '2022_01_08_1', '2022_01_08_3', '2022_01_08_4','2023_03_12_4']

3) filenames =
['2021_05_25_1','2021_08_23_1','2022_12_01_4','2022_05_17_1','2022_05_17_3','2022_05_17_4', '2022_05_16_2','2022_05_16_3','2022_05_16_4','2022_05_15_4', '2022_06_07_1', '2022_05_02_3']

4) We did not do further analysis on this case in Appendix B, hence we use the results from one value per track for the drawing below.
filenames =
['2022_01_04_1','2022_01_04_3','2022_01_04_4','2022_05_27_3','2022_05_27_4','2022_08_23_3']

Although the curve fits describe well the distribution of EDR in the area, as well as change with direction or overall windspeed, they are not capturing well extreme values that deviate much from the EDR averages. These extreme values may cause severe turbulence, even when the averages do not, this is addressed further in Appendix G.

Low windspeed (Thermic): Three measurement dates, one with three concurrent flights, one with two simultaneous flights and a single track. The visual similarity of below pictures encourages combining the measurements for one view and curve fit. Results are presented below. Also, we pull out the vertical measured distribution of EDR in two places (at the mast and Lidar sites).
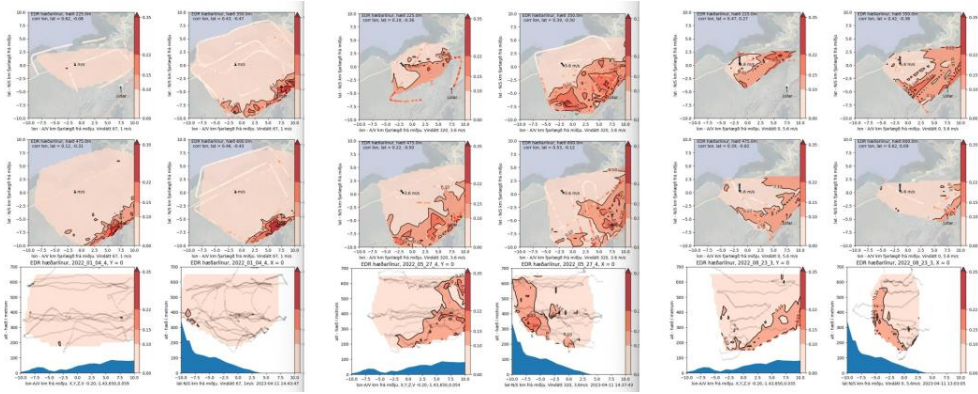
a,b,c,d,e,f,g = 3.900e-03 -6.639e-03 8.049e-09 -7.687e-05 6.809e-02 5.436e-03 6.810e-05
A total of 18000 datapoints, and correlation coefficient r = 0.74.
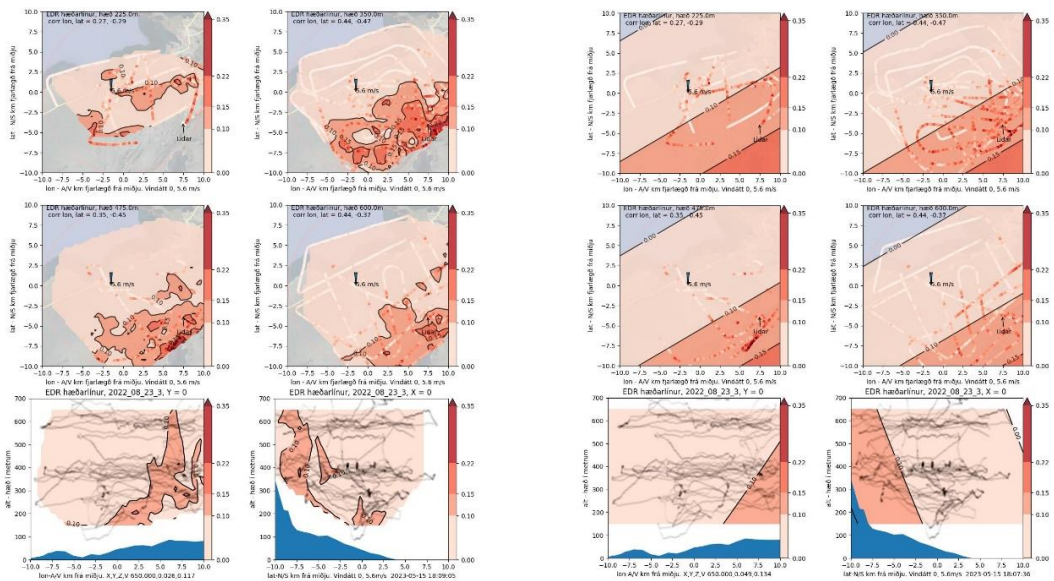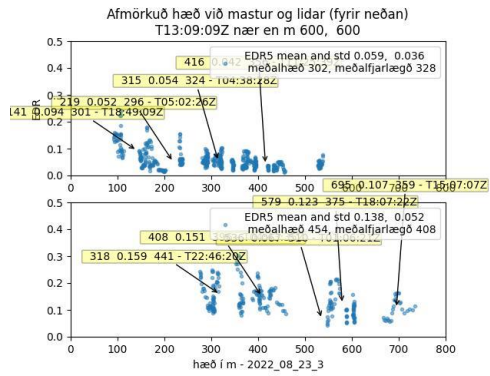
Wind 20 - 80 degrees: 11 files used with 34000 measurements, average windspeed of 8.1 m/s, average direction 40 degrees. (adding the measurements at 87 deg (2022_05_17)) to the data pool diminishes the correlation, hence the 87 degrees are kept in the last group). The curve fit can be used to estimate EDR by inserting wind speed and direction. As an example, 8.1 m/s from 40 degrees result in EDR 0.14 at 300 m over mast, and the average of the direct measurements there yielded 0.14. Note, these are estimating 20 s averages.

Similar exercise for the location marked Lidar yields at 40 degrees wind of 8.1 m/s; 0.18 compared to 0.19 measured. Picture below shows EDR 5 s, EDR 20 s, Case 2 correlation for EDR20 and measurements in vicinity of mast and lidar.
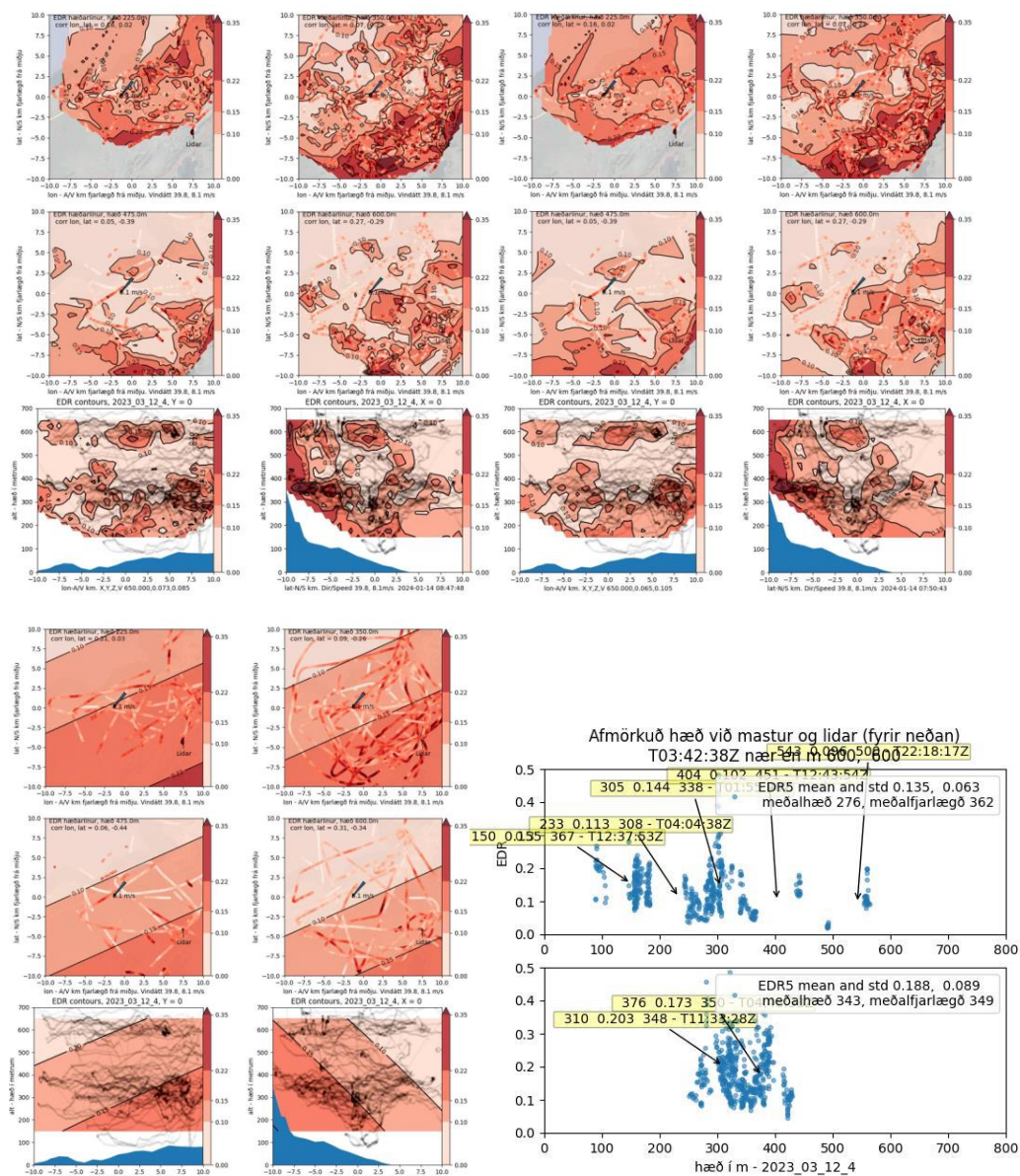
Wind 80-180 degrees: 12 files with 28000 datapoints, average windspeed of 8.6 m/s, average direction 116 degrees. Wind 116 degrees at 8.6 m/s yields from correlation EDR20 of 0.18 at mast, and 0.22 at Lidar, which compares well with the direct measurements of 0.18 and 0.24 below.
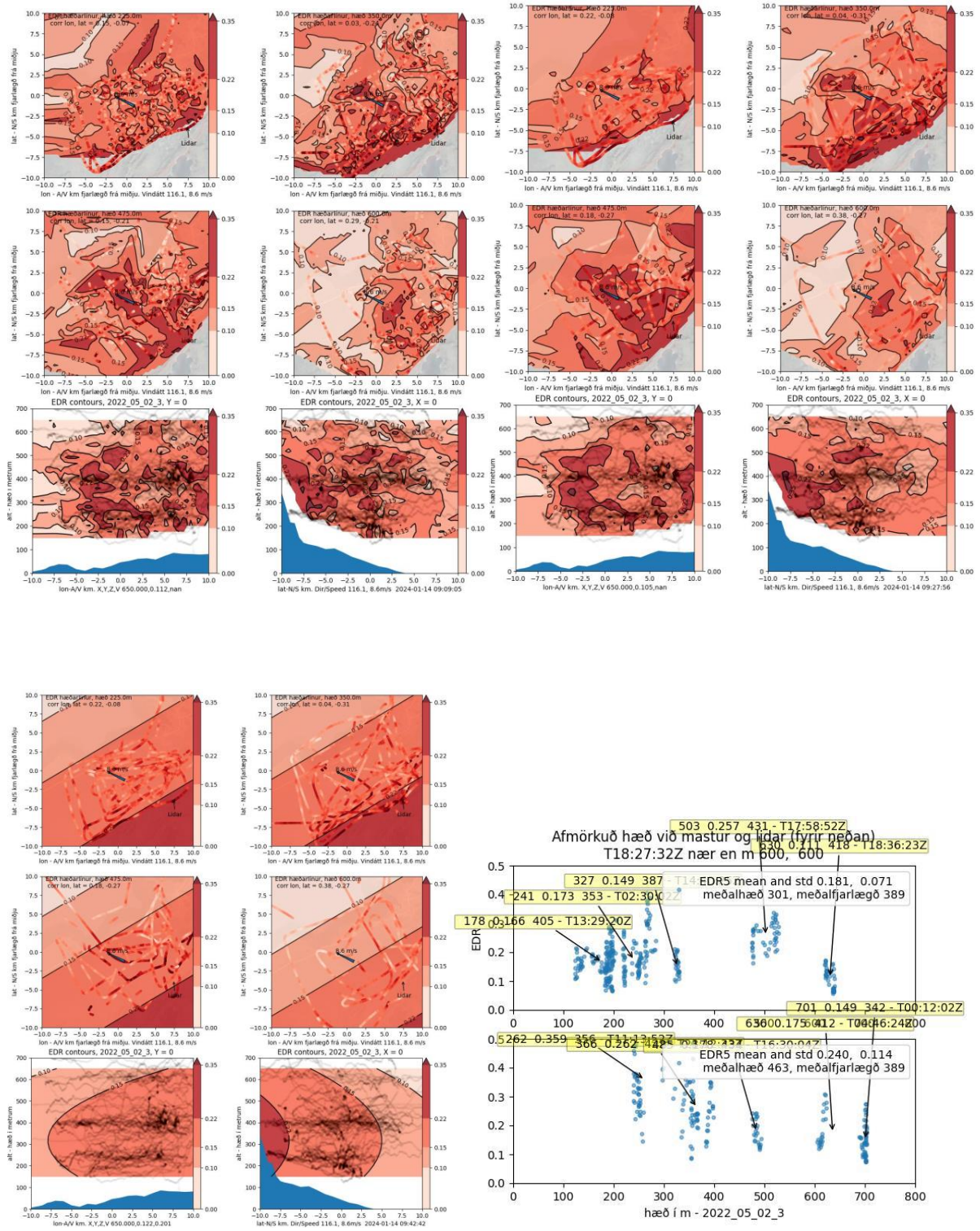
Appendix F: Dash 8 Missions.

A DHC8-200 aircraft based at Reykjavik airport was recruited as a platform to further strengthen the foundation for measurement data. The purpose of the Dash 8 missions can be divided in two parts:

1. Capability for measurements in weather conditions (wind speeds, turbulence levels) more adverse than attainable by the main measurement platform, the Savannah aircraft. The resultant data should complement other acquired data to enhance the measurement database.
2. Demonstration of the capability of the modelling and data acquisition methods to capture the same results in terms of EDR within a particular turbulence field, irrespective of the aircraft type used, size or airspeed.

The intended mission for the D8 was primarily to acquire data during weather conditions unattainable by the Savannah aircraft. As such, the preferable wind conditions for a D8 mission would be when wind direction in Hvassahraun is in the sector from 090° to 210° with mean wind speeds over 15 m/s. However, it was decided that before attempting such a flight, the measurement platform would need to be tested in easier conditions similar to those experienced by a Savannah aircraft during a typical measurement mission. An additional benefit of such flight would be the possibility to compare the results with results of a Savannah flight in similar conditions. It was decided that the intended flight track should include the following:

1. An approach to approximately 600 feet AGL and a missed approach to a fictional E, SE and S runways at Hvassahraun.
2. An approach to minima and missed approach to the runway in use at Reykjavik and Keflavik, for comparison purposes.
3. Data acquisition at different altitudes within the defined area of interest in Hvassahraun.

Image XXX below shows a typical flight track as designed to incorporate goals 1 to 3 above, prior to the D8 missions.
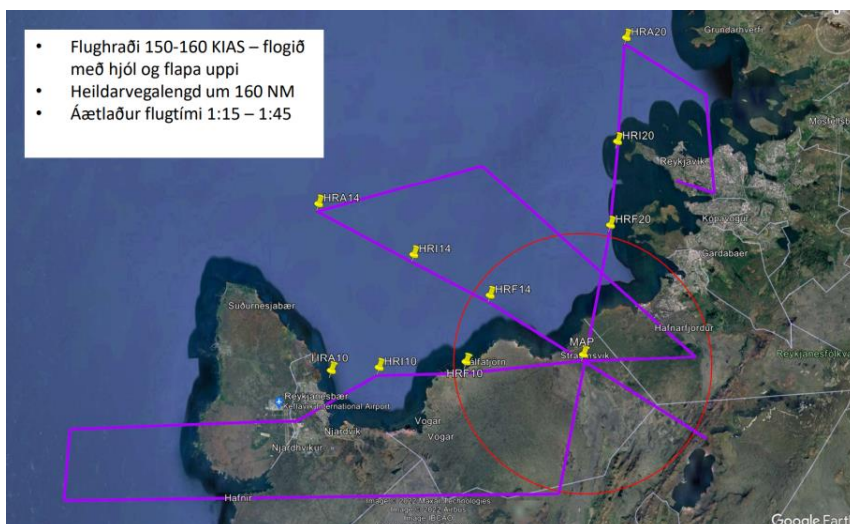
The aircraft operator defined a list of limitations and guidelines to be followed during any measurement flight in order to mitigate risk of unwanted events. The limits related to weather conditions were set as follows:

1. Maintain visual meteorological conditions (VMC).
2. Wind gusts at Reykjavik airport below 40 kts.
3. Flight performed in daylight.

During the data acquisition phase of this study, it was unfortunately only possible to apply the D8 aircraft on two occasions, of which the purpose of the first flight was to test the platform, find the most appropriate locations for the sensors and for the flight crew to practice the intended flight track. The second flight was planned to be performed in a SE wind direction with speeds over 15 m/s, however the departure was delayed due to uncontrollable causes. When the flight was finally performed, the wind had veered to a more southerly direction and the wind speeds had slowed to 12 m/s. An overview of the wind conditions during the D8 missions are stipulated in table XXX below:

Date and time	Mean Wind Direction @HVH:	Mean Wind Speed @HVH:
2022-11-06, 11:00 UTC	060°	6 m/s
2022-12-01, 16:00 UTC	170°	12 m/s

The Dash 8 flights were conducted with 4 sensors, of which 2 were placed in the Flight Deck and the other two in the cabin, one in the seat row as close to the center of gravity as possible and the other in the aftmost seat row. The GPS sensors were positioned in the respective seat row windows. The modelling data used for the Dash 8-200 aircraft is listed in table XXX below:

Airspeed, typical approach [m/s]	55
Airspeed, typical cruise [m/s]	140
Mass range, in flight [kg]	12000 – 16919
Wing area [m2]	54.4
Aspect ratio	13.8

3.2.1. Mission Results

DHC8 Mission #1

Date: 06-Nov-2022

Aircraft: TF-FXH

Pilot/Co-pilot: Jonas Jonasson / Kristjan Magnusson

Purpose: To test the DHC8 as a sensor platform, practice flight tracks including approach to three fictional runways, find optimum placements for sensors and to fly in conditions similar to smaller aircraft to verify the modelling methodology.

Weather conditions: Wind from northeast, 6 m/s. Dry weather, visibility more than 10 kilometers and no cloud below minimum sector altitude.

Flight duration: 1 hr 20 min, takeoff at 11:07 GMT.

It was decided to place 2 sensors in the flight deck, one on each side of the glareshield as close to the longitudinal axis of the aircraft as possible. The third sensor was mounted on seat armrest as close to the center of gravity point of the aircraft as possible. The GPS sensor was placed in the adjacent window to ensure proper connection. The fourth and last sensor was placed similarly, but in the aftmost seat of the cabin.

Figure XX shows the flight track and the vertical profile is shown in figure XXX. Figure XXX is a visualization of the measured turbulence at each point along the route. From the latter figure it can be concluded that the highest turbulence is measured on the leeward side of the mountain ridge, intensifying as the aircraft is flown closer to the ridge. Another interpretation is that of the three approach courses flown, the highest turbulence was measured during the missed approach segment of the southeast runway (runway 14).

Figure 1: DHC8 mission#1 horizontal profile
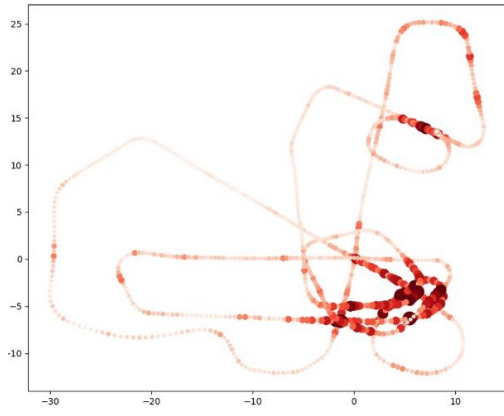
Figure 2: D8#1: Calculated EDR along horizontal profile

This interpretation is further visualized in figure XX, which shows the resultant area contour plot after data from sensor 3 has been processed (all altitudes). These results are also in line with other data acquired in similar weather conditions with smaller aircraft.
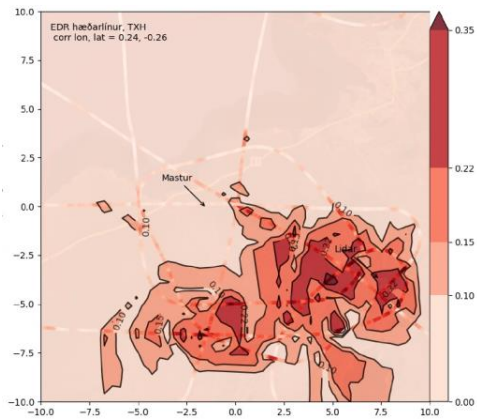
Figure 3: D8#1 EDR Contour Plot

In general the sensor measurements agreed well, however a difference of 10-20% in RMS vertical acceleration was observed between locations, with the highest values observed at the aftmost station, but the lowest values on the sensors that were placed in the flight deck.

In this report, only data from sensor #3 (closest to the center of gravity) is used.

It is reassuring to see how well the results of this measurement flight resembles the results of a 3 aircraft measurement flight that was performed in similar weather conditions (northeasterly wind, 8 m/s) on January 8th 2022. These similar results from similar weather conditions, but with two very different aircraft indicate that the modelling methodology is sound. A visual comparison can be observed in figures XXX to XXX below. Better horizontal and vertical track coverage of the measurement area of the three aircraft mission leads to higher resolution contour plot, but the resemblance is best conveyed by looking at the peak EDR values and locations.
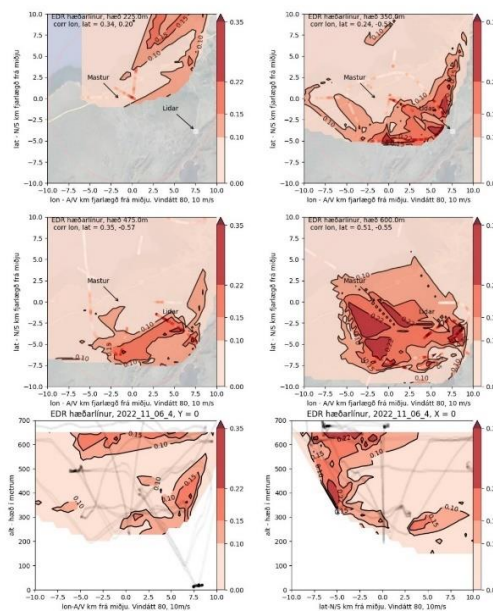
Figure 4: Dash 8 6.11.2022
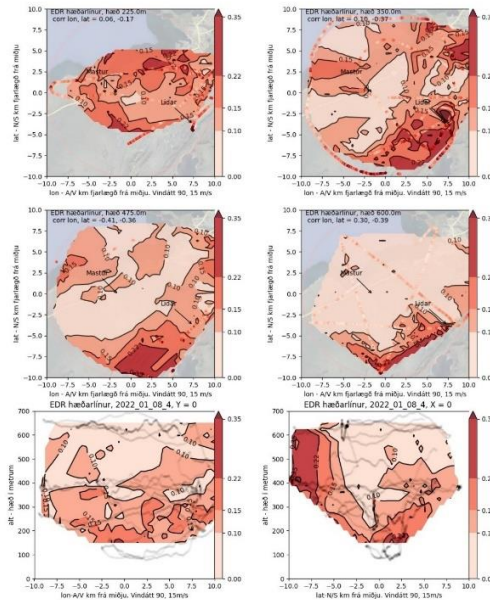
Figure 5: Three aircraft mission 8.1.2022

Another method to evaluate the similarity of the measured turbulence state between the two measurement missions is to use linear regression (see CHAPTER XXXX). *The results of the approximation constants are summarized in table XXXX below.* The regression data from both flights are normalized at wind direction 045° with wind strength at 7 m/s in figures XXX. Similar to the visual comparison of the contour plots, the same trend can be observed:

1. The area EDR values increase to the southeast (towards the mountain ridges)
2. EDR values have a vertical maximum close to or at the height of the mountain ridges.
3. Both EDR fields (D8 and 3 aircraft) are similar with respect to 1) and 2), and with respect to estimated local absolute values of EDR:
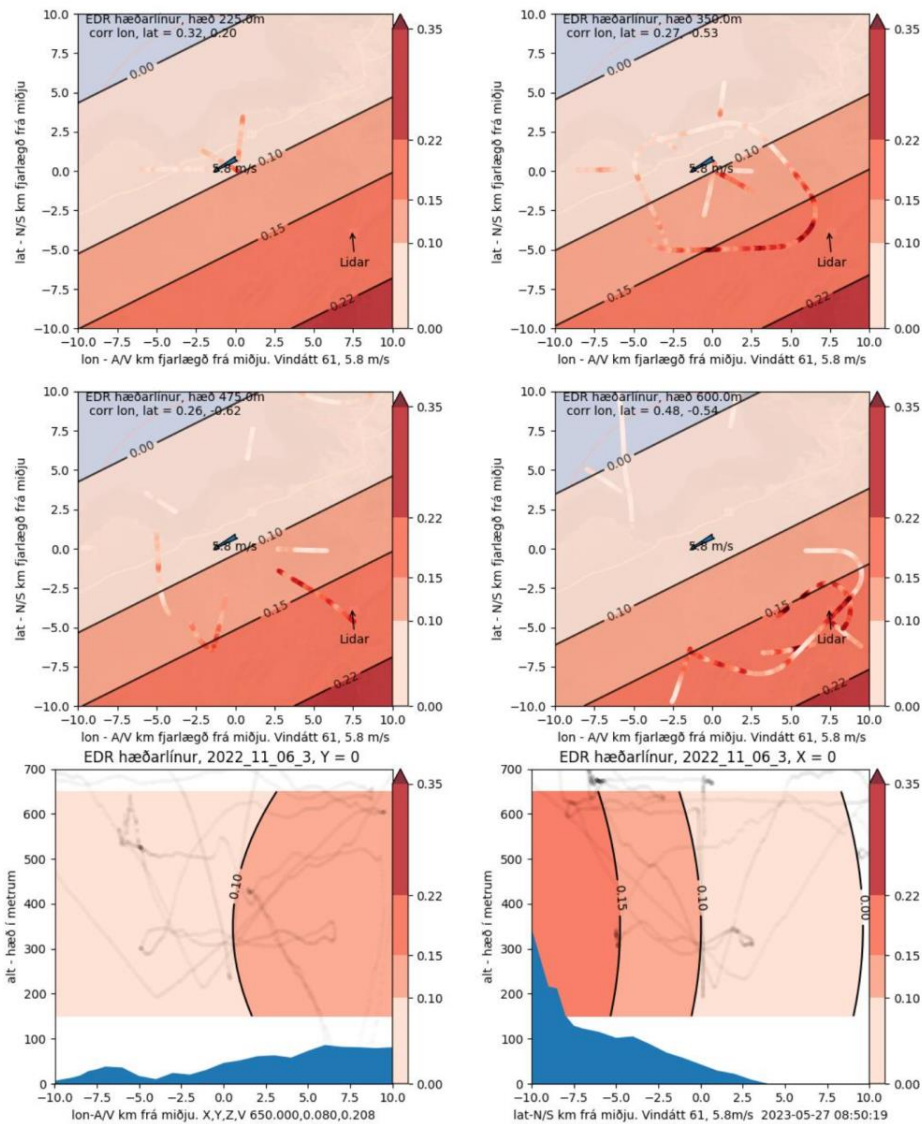
Figure 6: Dash 8 (06.11.2022) regression
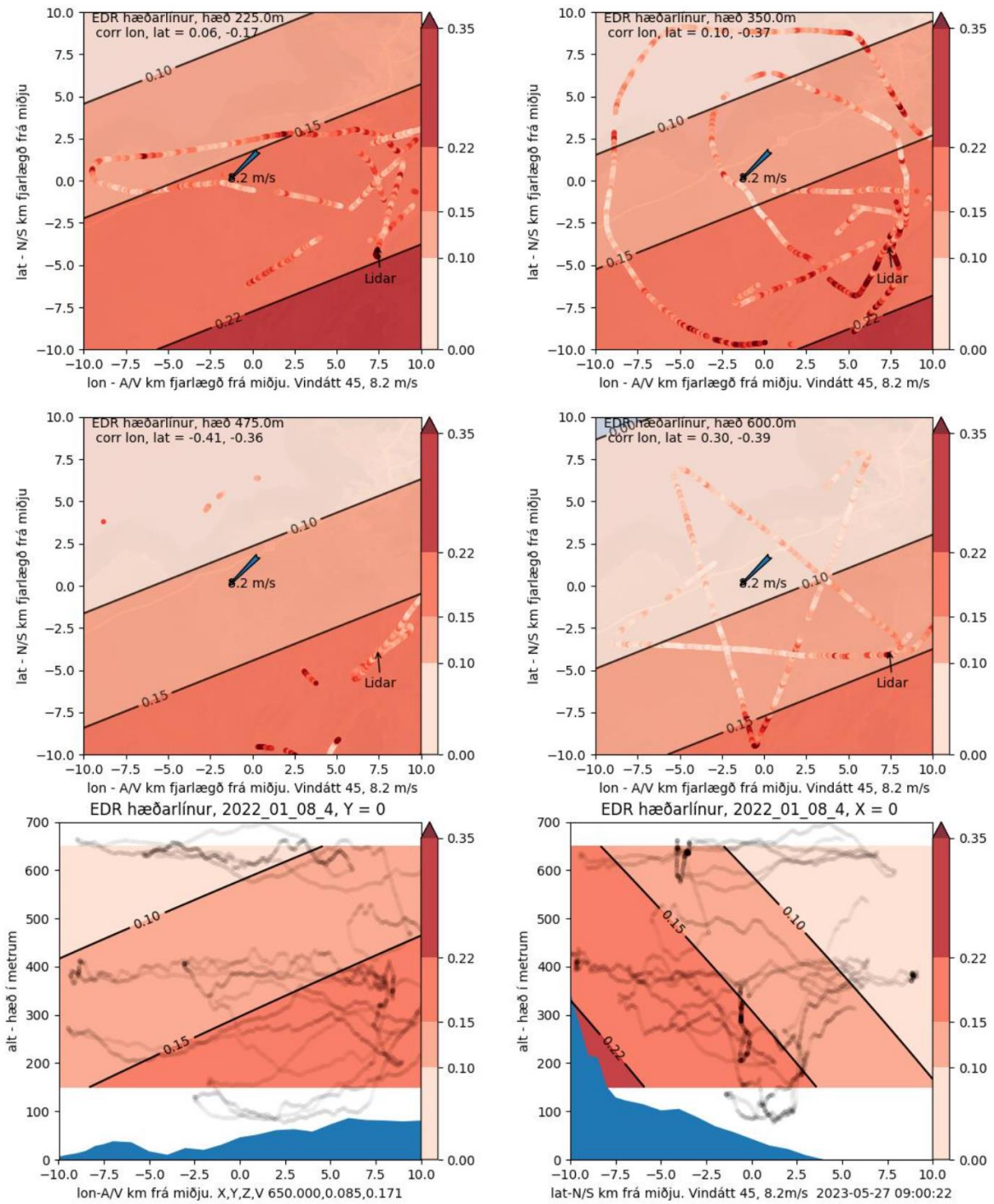
Figure 7: Three aircraft regression (08.01.2022)

The measured data from similar wind conditions can be combined to obtain a statistically improved model of the area EDR field, even when data is acquired using very different aircraft (size, speed, mass). An example is seen here below. Here all collected data when mast wind is between 0 and 70 deg, over 5

m/s is combined in a statistical model. As before, the results are based on wind blowing from 45 degress at 7 m/s. Once again, the same general trend is observed. Note that the track lines in the figures are a representation of the actual track flown thus representing the density of the data pool. For this particular dataset, multiple measurements flights flown in similar conditions are combined to give the below results, which explains the busy trackline traffic.
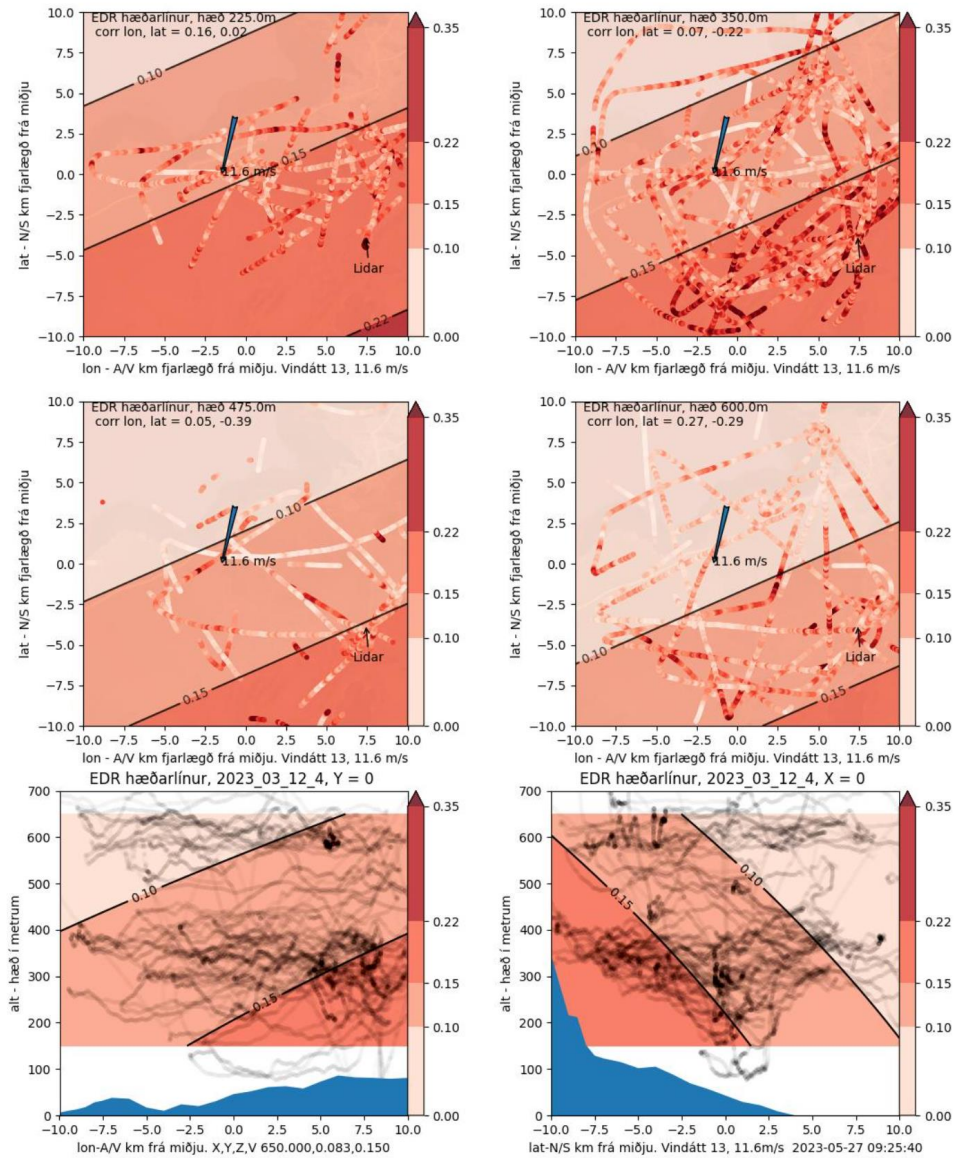
Figure 8: Combined data (all 0-70deg >5m/s)

DHC8 Mission #2.

Date: 01-Dec-2022

Aircraft: TF-FXH

Pilot/Co-pilot: Jonas Jonasson / Kristjan Magnusson

Purpose: To perform a measurement flight in conditions not reasonably achievable by smaller aircraft. Perform approaches to KEF and RKV airports for comparison purposes.

Weather conditions: South-southeasterly, 12 m/s. Visibility more than 10 kilometers. Light showers of rain, clouds broken between 3000 and 4000 feet.

Flight duration: 1 hr 8 mins, Takeoff at 15:40 GMT.

The ability of the DHC8 aircraft to handle more adverse weather than the smaller aircraft is desirable from a data collection standpoint, as it is possible to extend the data pool to higher average wind speeds. This injection of otherwise out-of-reach data further improve the statistical modelling of the area EDR field and has the potential to identify special circumstances that potentially are only observed in high wind conditions that are not accessible to small aircraft.

The sensor setup during this flight was identical to mission #1 and the sensor located closest to the center of gravity (sensor #3) is used to display the results.

The original intend for this mission was to collect data during a SE wind with wind speeds over 15 m/s. However due to uncontrollable causes the departure of the flight was delayed and when airborne, the wind had veered to a more southerly direction and wind speed had slowed to 12 m/s.

Figures XXX and XXX show the horizontal and vertical profile of the flight respectively. To summarize, the flight began with approaches to the fictional southerly runways at Hvassahraun followed by missed approach procedures (runways 20 and 14). Next, data was collected by flight at approximately 1500 feet AMSL inside the play area after which a low approach to Runway 19 at KEF airport was performed. After the missed approach procedure from KEF, the course was set to follow the mountain ridges to the east close to 500 feet AGL followed by a low approach to runway 19 in RKV. After the missed approach procedure the flight concluded with a landing on the same runway.

Figure 9: DHC8 Mission#2 horizontal profile

Figure 10: DHC8 mission#2 vertical profile
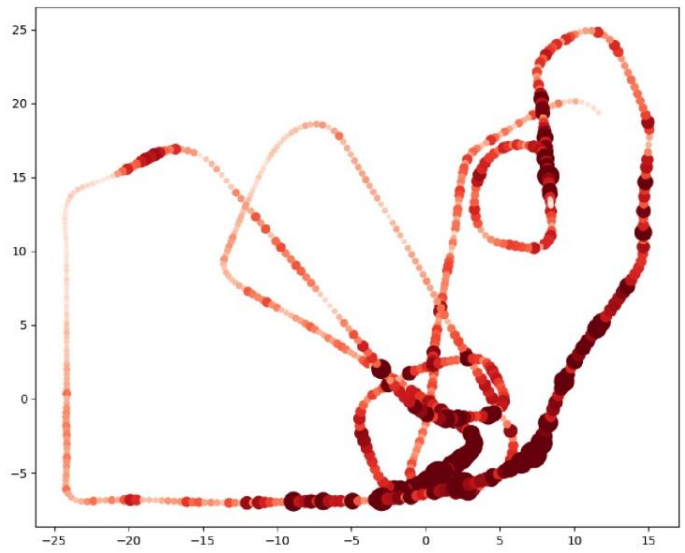
Figure 11: D8#2 Calculated EDR along track
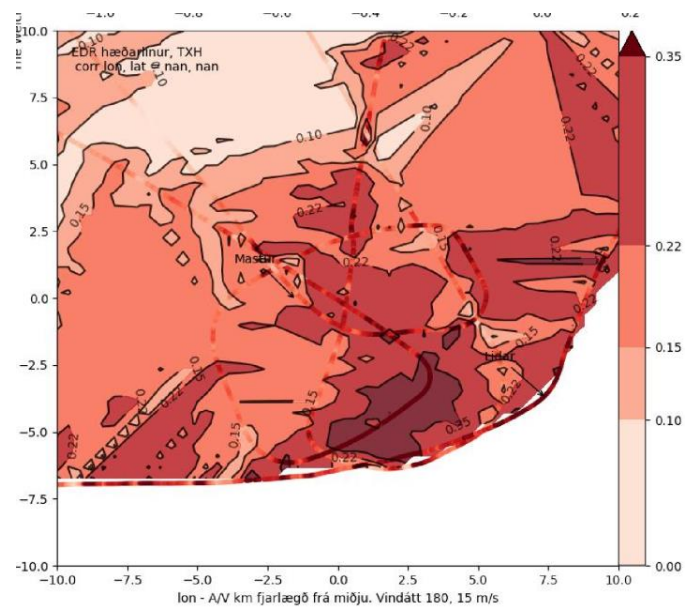
Figure 12: D8#2 EDR Contour Plot

Appendix G: Statistics of vertical accelerations.

Our estimates of EDR in Hvassahraun come from measuring vertical accelerations and motivated by Bowles et al NASA/CR-2009-215769, use mainly gRMS5, a 5 second RMS rolling average for variation in g from the level flight 1g. In their report they stated that they chose 5 sec based on *"The need to balance between 1) a sample window small enough to adequately resolve small scale turbulence that affect aircraft through induced g-loads and 2) an accelerometer measurement sample size large enough to calculate an RMS with acceptably small random error"*. They further concluded that the gRMS5 could also be a surrogate for peak acceleration. Peak acceleration is the load that causes structural damage and/or injuries to crew or passengers. They developed the following chart, marking also their limits for moderate, severe and extreme levels of turbulence:
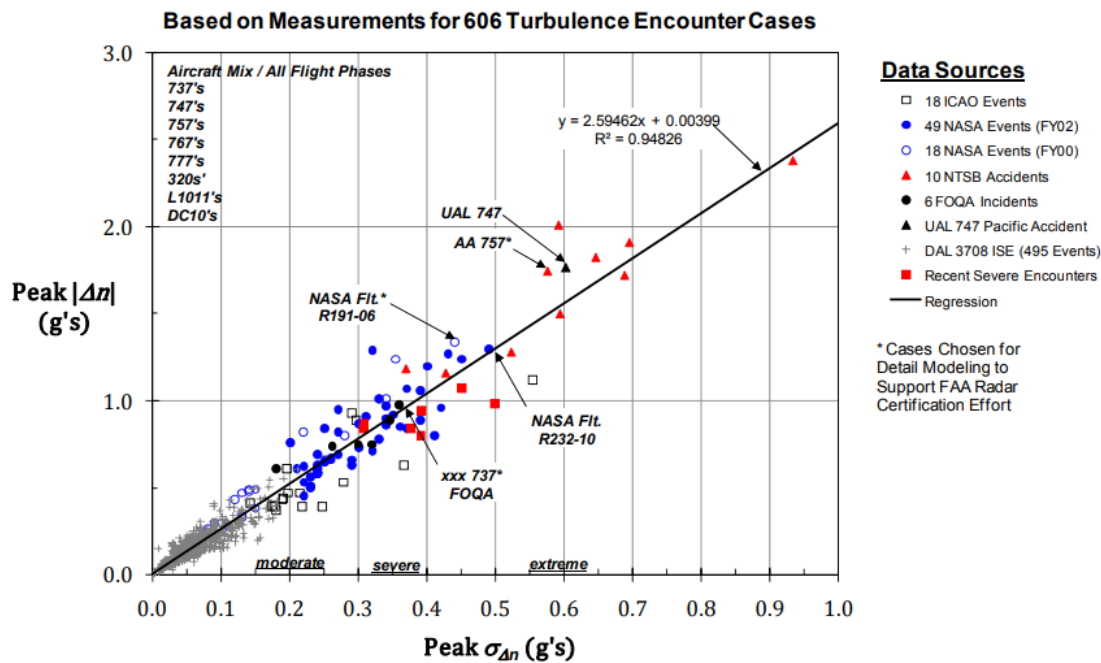
Figure 2: Correlation between Peak Load and Peak $\sigma_{\Delta n}$ (5 sec. window)

Main conclusion is that peak acceleration is roughly 2.6 times the RMS5 value.

Our data calculates gRMS from data collected at 200 hz and bandpass filtered. We calculate the 5 sec gRMS from 1000 measurements and keep the peak value in each ensemble to plot peak vs. gRMS. Below we have several plots with 5 sec gRMS (x-axis) and peak value.
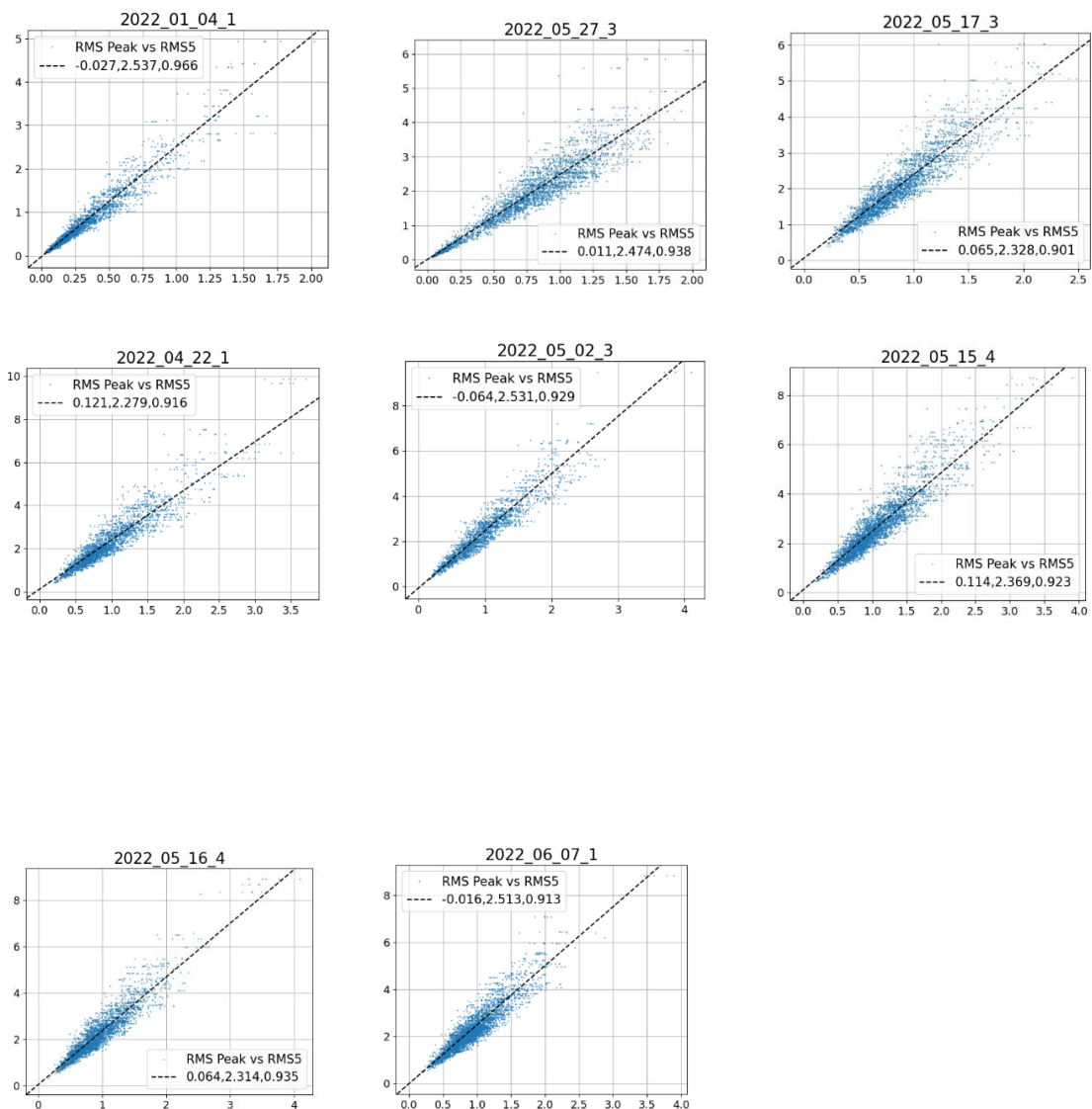
Through curve fitting we get the factor between 2.3 and 2.5 for various wind conditions in the Hvassahraun area, which is in good agreement with the values from the NASA report.

Now, as the fluctuations in g leading to the calculated gRMS can be assumed Gaussian (a quick look at data indicates this also), and if 1 g is removed from the measurements, the fraction of measurements exceeding certain values (i.e. the peak) can be evaluated. For a Gaussian (Normal distribution) the following table does apply:

RMS (number of sigma)	% exceeding value
1.00	31.7
1.65	10.0
2.00	4.55
2.5	1.24
3.00	0.30

3.30	0.10

This means for example that 1.24% of measurements should be expected to exceed 2.5 x gRMS which is represented by the slope of the line 2.5 in our graphs above. And one can expect that taking a longer period than 5 sec would deliver a higher multiplier for the peak value.

We can do the above exercise again on our data to look for peak and 90th percentile value for various averaging periods (1sec, 5, 20 and 60). We do this here for three different flights, and plot the distribution of calculated RMS. The RMS represents variance of a Gaussian curve, but its values change during a measurement flight when the aircraft moves from one place to another. The distribution of its values resembles Weibull distribution:
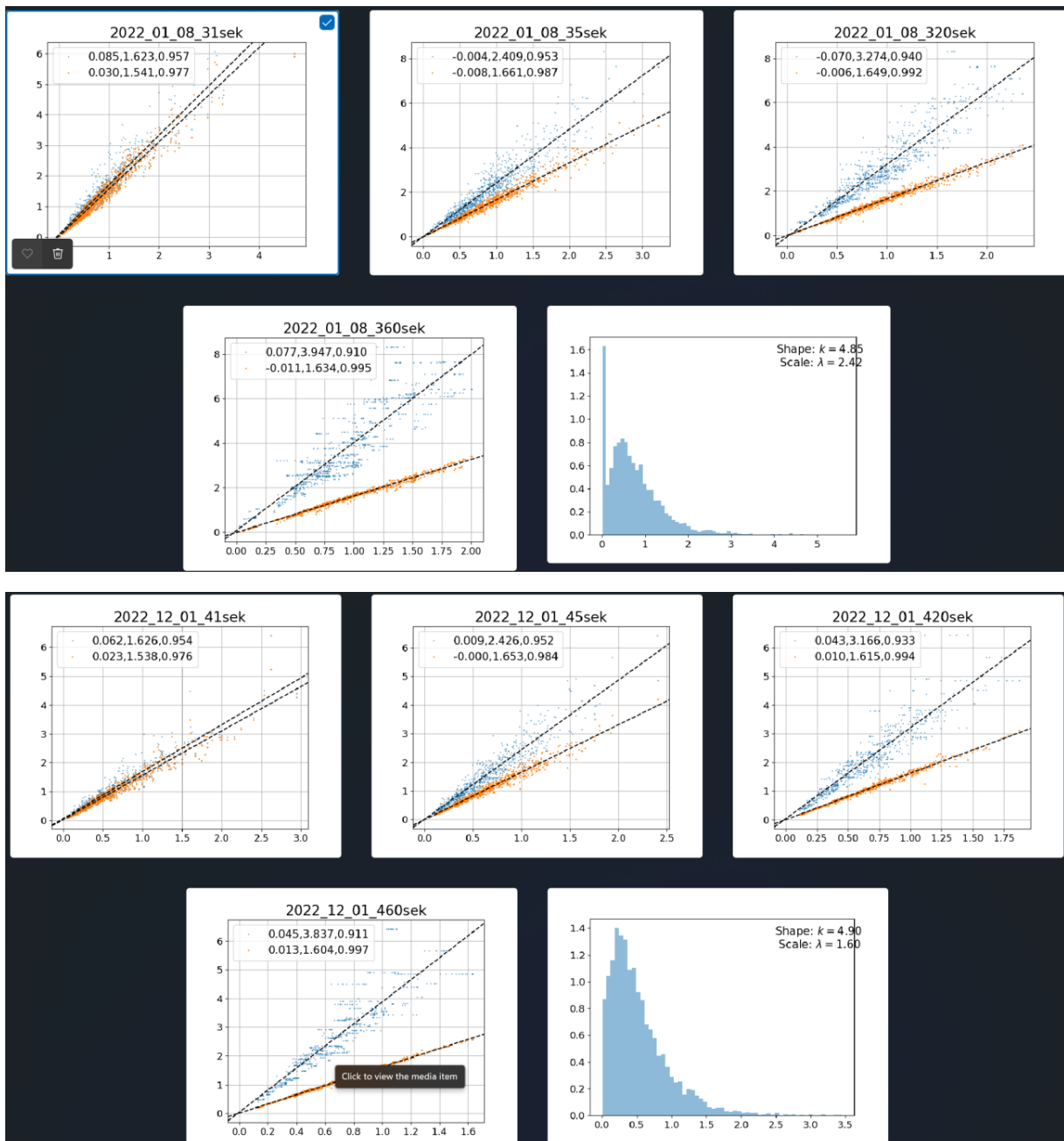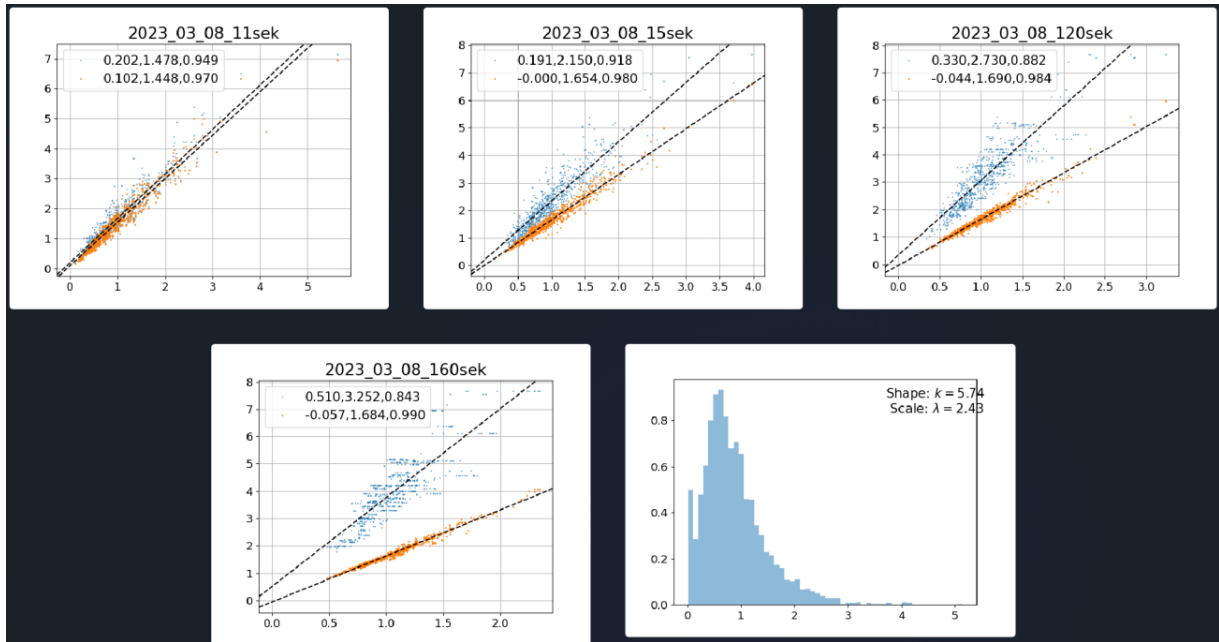
The 90th percentile is insensitive to the averaging period, pretty much 1.6 as expected. But the peak value (the slope of the plot average to peak) is sensitive to the period. At 1 sec, the peak value is one out of a total of 200 measurements, or 0.5%, and a typical slope is just a bit higher than the 90th percentile slope. At 5 sec (peak value 1/1000) it is 2.5 (see table above, and comparison to Figure 2 from the NASA report). One should expect the slope to increase as data further out on the tail of the Normal curve is brought into play; At 20 sec, (peak is 1 out of 4000 measurements), slope is close to 3 as expected. And, finally, 60s (1/12000), the slope approaches 4, indicating a measured peak at close to 4 x variance.

This allows us to examine table 2 from Aviation Turbulence:

Table 1.1 Turbulence reporting criteria and approximate atmospheric turbulence levels

Description	Aircraft-dependent measures		Peak normal accel (g)[b]	RMS normal accel (g)[c]	Atmospheric measures	
	Aircraft reaction[a]	Reaction inside aircraft[a]			U_{de} (m s^{-1})[d]	$\varepsilon^{1/3}$ (m$^{2/3}$ s^{-1})[e]
Light	Turbulence that momentarily causes slight, erratic changes in altitude and/or attitude (pitch, roll, yaw). or Turbulence that causes slight, rapid, and somewhat rhythmic bumpiness without appreciable changes in altitude or attitude ("chop").	Occupants may feel a slight strain against seat belts or shoulder straps. Unsecured objects may be displaced slightly. Food service may be conducted and little or no difficulty is encountered in walking.	0.2–0.5	0.1–0.2	2.0–4.5	0.1–0.39 (0.1–0.21)
Moderate	Turbulence that is similar to light turbulence but of greater intensity. Changes in altitude and/or attitude occur but the aircraft remains in positive control at all times. It usually causes variations in indicated airspeed. or Turbulence that is similar to light chop but of greater intensity. It causes rapid bumps or jolts without appreciable changes in aircraft altitude or attitude.	Occupants feel definite strains against seat belts or shoulder straps. Unsecured objects are dislodged. Food service and walking are difficult.	0.5–1.0	0.2–0.3	4.5–9.0	0.40–0.69 (0.22–0.47)
Severe	Turbulence that causes large, abrupt changes in altitude and/or attitude. It usually causes large variations in indicated airspeed. Aircraft may be momentarily out of control.	Occupants are forced violently against seat belts or shoulder straps. Unsecured objects are tossed about. Food Service and walking are impossible.	1.0–2.0	0.3–0.6	≥9.0	≥0.70 (≥0.48)
Extreme	Turbulence in which the aircraft is violently tossed about and is practically impossible to control. It may cause structural damage.	Not defined	≥2.0	≥0.6		

[a]FAA (2014), Table 7-1-10
[b]E.g., Lee et al. (1984), Lester (1993), Fig. 1-8
[c]Bowles et al. (2009) based on running 5-s window
[d]Gill (2014)
[e]Peak over 1 min. ICAO (2013) definitions, updated values by Sharman et al. (2014) in parentheses

1 Nature of Aviation Turbulence

7

For severe turbulence (gRMS=0.3 g or roughly 3m/s^2, peak=1 g). The peak roughly 3.3 x gRMS is in line with the above analysis and Normal distribution, i.e. with gRMS of 0.3 g, you will experience instances with peak acceleration of 1 g.

The table also has severe turbulence at DEVG over 9m/s. However, Soo-Hyun Kim et al (2016) investigated this thoroughly with data from Airbus and Boeing and came to the conclusion that severe turbulence occurred at EDR = 0.52 (DEVG=7.4), and EDR = 0.59 (DEVG = 5.24) respectively.

This is in fair agreement with the above table, but the EDR values in the table have been updated by ICAO such that severe EDR peak is now 0.45. The following notes from ICAO describe EDR:

 Note 1.— The EDR is an aircraft independent measure of turbulence. However, the relationship between the EDR value and the perception of turbulence is a function of aircraft type, and the mass, altitude, configuration and airspeed of the aircraft. The EDR values given above describe the severity levels for a medium-sized transport aircraft- under typical enroute conditions (i.e. altitude, airspeed- and weight).
Note 2.— EDR refers to the cube root of the energy or eddy dissipation rate estimated from aircraft data parameters (e.g., vertical wind velocity or aircraft vertical acceleration).

Appendix H: Simulation of Aircraft Turbulence Response

H.1   General Introduction

The question arises as to how an airport, existing or planned in a new location can be assessed in terms of the turbulent conditions that exist at its location and in its vicinity. In this project it was decided to focus on the airport terminal area, which in Iceland is typically about 10 km (6 nautical miles) from the airport center-point up to an altitude of no more than 3 000 ft. This is the airspace that has been the primary airspace for carrying out in-flight acceleration measurements for evaluating the Hvassahraun site that is discussed in detail in Chapter 6 of this report. This has also led to the development of quantitative, statistical models that provide a reasonably accurate description of the intensity of the turbulence conditions in this volume of airspace. The models provide a means of determining the intensity of the vertical wind component in terms of EDR as a function of position, height and wind conditions. This permits vertical wind component data to be generated by the simulator that can be used to compute a corresponding time response, i.e. the acceleration, of an aircraft of a specified type on any specified flight profile within the model area. This can for example be used to explore the turbulence conditions on commonly used approach paths and climb-out profiles when the runway orientations are known as well as the wind conditions (strength and direction) in the terminal area. This would aid in determining the level and likelihood of reaching or exceeding specified turbulence limits for the types of aircraft using the airport on a regular basis.

Clearly it is not easy to define universally acceptable criteria in this field. However, there is one criterion which from an operational point of view is often referred to, i.e. the average vertical acceleration of 0.3 g which can be expected to result in peak acceleration of the order of 1 g or about 10 m/s^2. This limit is well understood inasmuch as the occurrence of 1 g causes unconstrained mass to be detached from its base and may result in injury to unrestrained aircraft occupants. Clearly the response of any aircraft will depend on its design as well as operational parameters. This is reflected by the G term in the plunge model of vertical motion which is commonly used for determining the response of aircraft to vertical wind disturbances caused by turbulence. This parameter defines the bandwidth of the vertical velocity of an aircraft driven by vertical air currents caused by turbulent air flow:

$$G = \frac{\rho}{2} \frac{V_a S C_{L\alpha}}{M}$$

In the SI units G is defined in terms of rad/s. The low frequency response of vertical gust wind at frequencies less than G, basically has a gain of 1.0 (0 dB) when the aircraft velocity is considered as an output. The aircraft "rides" the waves without any appreciable error in this frequency range. When the gust frequency reaches $\omega_0 = G$ the amplitude of the output has decreased by

1

approximately 30% and a negative phase shift of 45° is present at this frequency. This is defined as the limit of the bandwidth (half power). Higher frequencies are increasingly attenuated in amplitude with the phase shift eventually approaching - 90°.

The bandwidth of the aircraft, i.e. G, changes linearly with true airspeed V_a. This leads to an increased sensitivity to vertical gusts as the aircraft responds more to higher frequencies of the vertical wind component. Conversely the response can be reduced by slowing down, i.e. by decreasing the bandwidth of the aircraft response. However, it must be taken into account that the turbulence power spectrum which is defined in terms of wave number is also subject to changes with air speed.

H.2   Simulation Tool for Turbulence Assessment

The primary purpose of the simulator in this project is to provide a tool for generating a detailed dynamic response of an aircraft of a specified type to vertical air turbulence. This is done by computing the time histories of the vertical acceleration, vertical velocity, and other state variables of the aircraft as well as the generating the disturbance velocity in terms of a temporal vertical wind component. The simulator which has been developed for this purpose is made up of the following elements which are shown in Fig. H-1, including:

- Model for generating the vertical wind component, w_g, which subjects the aircraft to vertical forces developed by the wings in level flight, as a function of time;

- Aircraft model that computes the aerodynamic forces acting on the aircraft resulting in the acceleration and other dynamic variables that describe its vertical motion;

- Measurement modules that mimic the methods used for in-flight measurement processing using simulated acceleration as input.

- Modulator which provides the capability for generating time variant wind with specified EDR obtained from EDR data derived from in-flight measurements, model data such as the correlation models developed in this project, or any other source of EDR data;

- Flight Profile Generator is a non-dynamic software module that computes a ground track and altitude profile that is "flown" on a prescribed route through the area under consideration, i.e. the Hvassahraun area. The profile is a three dimensional (x,y,h) series of coordinates with a time stamp that can be used to look up a model EDR value for each point. Such a profile, including time stamps, exists of course for any measurement flight recorded by the GPS unit associated with each acceleration measurement unit.
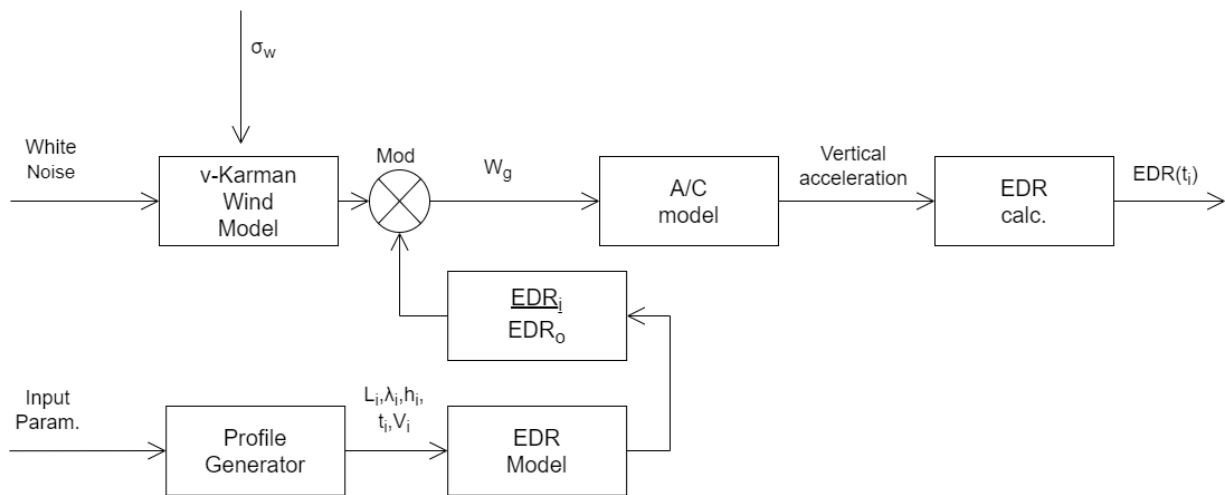
Figure H-1. Configuration of the Turbulence Flight Simulator

The general wind model, which is based on the von Karman power spectrum of air turbulence, is a time invariant stochastic process that is implemented by a linear shaping filter driven by a white noise input signal. This means that the statistical properties of the process, EDR included, are constant. Also, the process is ergodic so that statistical parameters can be determined by computing time averages.

The aircraft model is the plunge model that considers the aircraft to be a point mass that is subject to aerodynamic forces created by the wings. In addition to the typical lift equation the unsteady aerodynamic effect described by Küssner and Wagner are taken into account. Despite its simplicity the plunge model does express the essential response characteristics of an airplane to the vertical wind variations that provide the input signal to the airplane transfer function. This varies in accordance with the aerodynamic and other properties of the type of aircraft being modeled. The acceleration time response, provided by the simulator, is processed through a Butterworth band-pass filter, identical to the one used for processing in-flight measurement data. This is subsequently used to compute the estimated EDR. The filter parameters can be varied as required. Further information about the basic simulation package can be found in report on the pilot project undertaken in the first year of the Hvassahraun meteorological research program[1].

The modulator provides the means for accommodating the fact that the real turbulence process is neither time invariant nor stationary. On the contrary, EDR, which specifies the strength of the turbulence, i.e. the vertical position of the von Karman power spectrum, varies throughout the passage of an aircraft through a given airspace. This can be clearly seen in Figs. 5-2 a) and b) which depict the EDR data obtained on a typical mission over the Hvassahraun range.

---

[1] **Mælingar á loftkviku yfir Hvassahrauni – forverkefni jan-sept 2021**; (In-flight Measurements of turbulence over Hvassahraun Site – Pilot Project, Nov 2021)
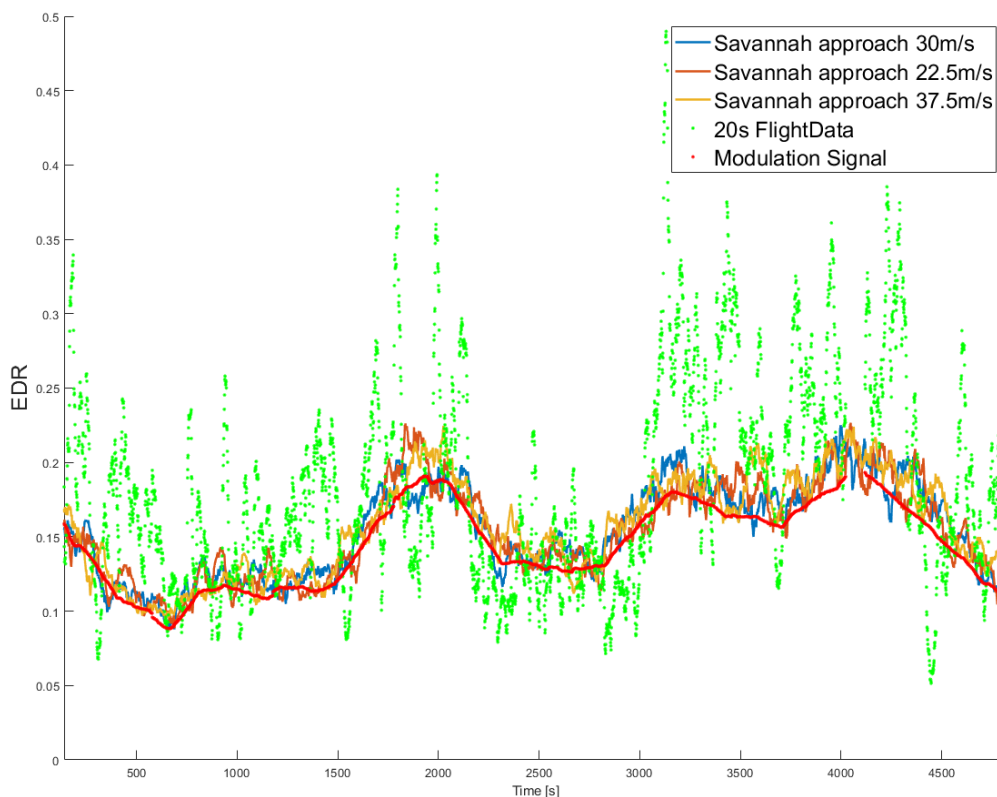
3

Figure H-2. Estimated EDR (blue, red and yellow graphs) obtained from simulated flights for three airspeed values (22.5, 30.0 and 37.5 m/s) of a Savannah measurement aircraft in the Hvassahraun area. Duration of each flight is approximately one and a half hours. The simulation is driven by the Case 2 correlation model (bold red graph) which was used to generate the vertical wind data for a profile flown on 29 December 2021. Also shown are the measured high frequency EDR estimates that are provided in green color. The EDR estimates that are obtained by the simulator are computed using simulated accelerations instead of actual measurements.

The EDR model results shown in Fig. H-2 (red graph) are generated from the model that is based on measurement data for Case 2 wind conditions. The model EDR data is computed using the coefficients of the appropriate model for the actual aircraft profile being analyzed. This profile, flown on 29 Dec. 2021, is followed through the area to generate simulated acceleration measurement which are sampled from the simulation stream. The EDR estimates are provided for comparison.

The simulated EDR data, depicted for three different Savannah airspeed values, appears to be very similar to the real EDR obtained on the same flight profile as can be seen in Fig. H-2. The slightly higher values obtained from the simulation results may indicate that some fine tuning of the aircraft model parameters may be in order.

4

H.3   Objectives of the Simulations

The basic purpose of carrying out simulation exercises in this project is to be able to reproduce the dynamical conditions that have been observed through measurements of turbulence by different types of moving platforms or from fixed locations. In the project described in this report the emphasis is clearly on in-flight measurements. These are of particular importance as they are obtained in locations under various meteorological conditions that can only be reached by air be they airplanes, drones, helicopters, or other types of aerial vehicles. The in-situ measurements are consequently essential for providing input for developing mathematical models of air turbulence in conjunction with measurements derived from ground-based instruments, e.g. met masts, lidars and possibly radar.

Simulations using stochastic models to produce samples of the vertical wind component that causes the vertical acceleration of the aircraft are useful in several ways. Thus, they can be used to:

1. Provide a means of testing the effect of turbulence for various types of aircraft under different operating conditions, including those whereby the constraints caused by theoretical assumptions are infringed to represent realistic conditions.

2. Compare measurement and data processing techniques to obtain estimates of the underlying system parameters, including the estimation of the air turbulence intensity, i.e. EDR.

3. Classification of airspace in terms of turbulence by simulating measurement flights that provides an alternative approach to interpolating the properties of turbulence models based on measurement data from in-situ missions. These are essentially simulated measurement missions that would provide the same type of data as actual missions using models, such as the correlation models developed in this project, to provide the turbulence intensity for driving the simulation.

4. Perform various studies that allow statistical qualities to be determined for various maneuvers and more complex operational scenarios. This could include various common or uncommon procedures to be studied.

H.4   Testing of Modulated Simulator

5

The simulation of the vertical turbulence intensity in the aviation industry is most often implemented by using an approximation of the von Karman power spectrum. Thus a rational transfer function has been defined which can be used as a shaping filter to approximate the power spectrum of a stochastic process having almost the same properties as the Karman power spectrum. Both models have the same stochastic properties of being gaussian and stationary, i.e. they reach a steady-state and their statistical behavior, including mean value and variance of the output are constant. The model used in this project is specified in reference [1][2] as a third-degree transfer function driven by unity uncorrelated white noise. Coefficients, that are in part dependent on the desired standard deviation of the output gust velocity, σ_{wg}, the true airspeed, V_{TAS}, of the aircraft under investigation and a reference wavelength, L_w, of the turbulence process are all constants during any exercise.

In the real world this is not the case i.e. the intensity of the turbulence process varies significantly even in a relatively small area such as is considered in the Hvassahraun project. Hence, it is essential that the simulation model be able to take this into account. This could be done in at least two different ways; on the one hand by changing the strength of the driving noise (or static gain of the shaping filter); and on the other hand, by modulating the output of the gust simulator by a simple gain variation of the output gust signal, taking advantage of the fact that EDR is a linear function of σ_{wg} and vice versa. The latter approach was chosen in this case as the changes in intensity take place without any interference of the core process, which remains stationary without any transient behavior of the shaping filter. The transients would take some time to settle, creating unwanted disturbances in the simulation. Instead, the change of the amplitude of the gust wind output is changed to a new intensity level through a gain change proportional to the variation of the "actual" EDR process that is being simulated.

The process can be seen from Figs. H-3 a), b), c) and d).

---

[2] **Mælingar á loftkviku yfir Hvassahrauni – forverkefni jan-sept 2021**; (In-flight Measurements of turbulence over Hvassahraun Site – Pilot Project, Nov 2021
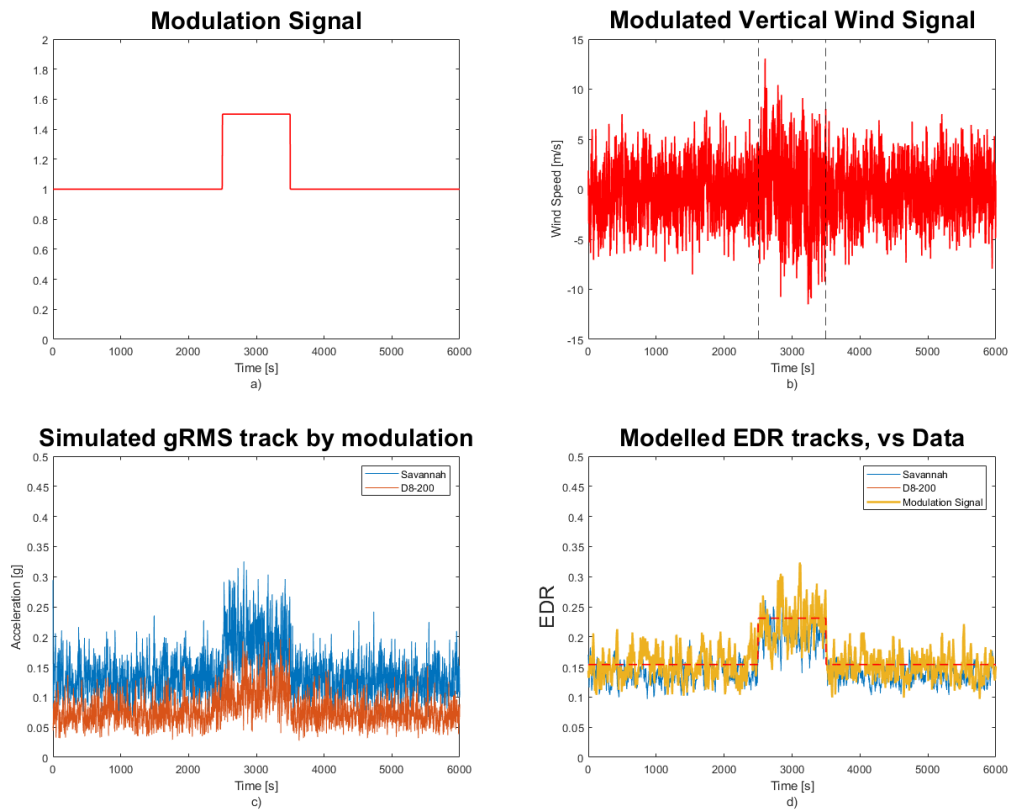
6

Figure H-3 a) Example of 50% step modulation signal b) Modulated Wind Signal of intensity σ_{wg} = 2m/s modulated between the dashed lines by 50%; c) corresponding increase in RMS acceleration from Savannah and D8 aircraft; d) corresponding "measured" EDR response (blue and yellow), compared with modulation test signal (dashed red).

The step changes that take place in this test are first and foremost used to demonstrate the capability of the simulator to respond to even abrupt changes in EDR. However, in practice, this will normally be a slowly varying change dependent on airspeed, aircraft heading and spatial and temporal EDR variations in the area. Only a part of the simulation capability has been exercised in the project described in this report. However, it is submitted that the capability of transforming the model information, described in chapter 4, into the time response of common aircraft types is very valuable for operational assessment of the turbulence environment of the model airspace such as the terminal area of an airport. A simulator, employing more advanced aircraft dynamical models would be a highly desirable improvement for this purpose.

7

Appendix I: Comparative Response of Aircraft Types

One of the primary roles of the simulator is to explore and demonstrate how aircraft of different types respond to turbulence. Table I.1 lists the types of aircraft as well as physical specifications and parameters relevant to the simulation of their responses to vertical air turbulence.

Table I.1 Specification of parameter values used for simulating aircraft responses for four classes of aircraft that can be expected to use Hvassahraun Airport

Aircraft - configuration	Air density (kg/m³)	Mass (kg)	Air Speed (m/s)	Wing surface area (m²)	$\frac{dC_L}{d\alpha}$ (deg⁻¹)	Mean chord length (m)	Conversion Factor* (m^{1/3}/s)	Bandpass filter window
Savannah final approach	1.225	450	30	12.9	4.77	1.4	5.1	0.1 – 2Hz
Savannah TA maneuver	1.225	450	60	12.9	4.77	1.4	9.8	0.1 – 2Hz
Dash 8-200 final approach	1.225	13,500	49	54.3	5.41	2.1	2.3	0.1 – 2Hz
Dash 8-200 TA maneuver	1.225	13,500	98	54.3	5.41	2.1	5.1	0.1 – 2Hz
King Air -200 final approach	1.225	4,673	50	28.2	5.22	1.7	3.2	0.1 – 2Hz
King Air -200 TA maneuver	1.225	4,673	100	28.2	5.22	1.7	6.8	0.1 – 2Hz
B737-9 final approach	1.225	61,000	71	127.0	5.25	4.6	1.9	0.1 – 2Hz
B737-9 TA maneuver	1.225	61,000	142	127.0	5.25	4.6	4.5	0.1 – 2Hz
B757-200 final approach	1.225	75,500	62	185.3	5.00	5.0	1.8	0.1 – 2Hz
B757-200 TA maneuver	1.225	75,500	124	185.3	5.00	5.0	4.2	0.1 – 2Hz

* Conversion of EDR to standard deviation of vertical acceleration for a given type of aircraft and its operational specifications. ** TA cruise: maneuvering airspeed in Terminal Area

I.1 Response of Individual Aircraft types

The following simulation "tests" are conducted separately for each type of aircraft which are all in either the approach mode (final approach airspeed) or a typical Terminal Area maneuver airspeed (double final approach airspeed) as defined for the five types of aircraft considered in Table 5.1. Each "flight" is carried out for a constant turbulence EDR to generate the vertical windspeed value. No EDR modulation is applied in this case so that the simulation reaches steady-state conditions as the initial transients are not included. This value is in all the simulated tests chosen as EDR = 0.4 $m^{2/3}$/s which is used for generating turbulent wind data to drive the simulation of the aircraft response in each case.[1] The output is primarily the acceleration level of each of these aircraft types at their specified airspeeds which are based on actual flight conditions during final approach at sea level and maneuvering at 2000 feet for each type. Subsequently, the ratios of the standard deviations of acceleration sequences are used for comparing the four types of aircraft considered in addition to the Savannah measurement aircraft which is by far the most responsive to air turbulence of the aircraft considered in this project. A rolling window of 20 seconds is used for all signal level RMS estimation calculations whereas estimates of standard deviations are obtained by averages taken over the full periods of the test runs.

Response of Beechcraft/Textron B-200

The Beechcraft B-200 is used extensively as an air ambulance aircraft in Iceland. It will typically be operating in conditions like the Dash-8-200, i.e. with frequent exposure to highly turbulent weather conditions and operation near its operational limits.

---

[1] A.C. de Bruin, H. Haverdings; **Validation of an Eddy Dissipation Rate Calculation Method based on Flight Data Recording Data,** National Aerospace Laboratory Report NLR-CR-2007-540, December 2007.
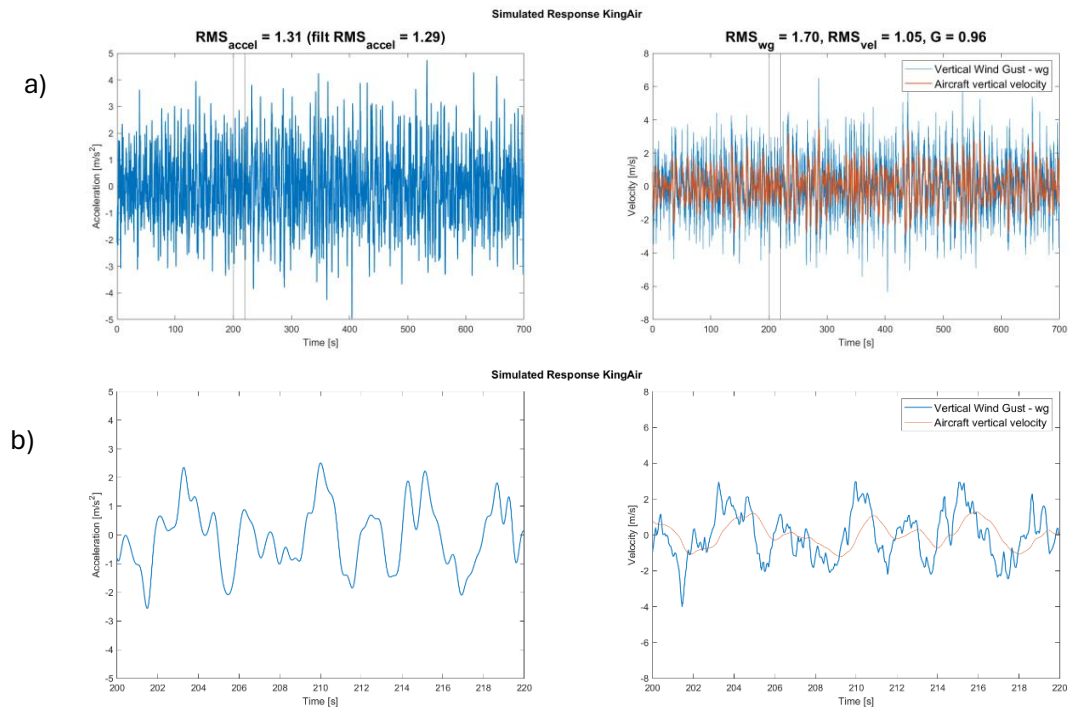
Figure I-1 a) Simulated response of the King Air aircraft at approach airspeed over a 700 second, 35 km flight segment. The vertical wind intensity is set for EDR = 0.4 resulting in vertical acceleration of RMS 1.3 m/s². The corresponding RMS vertical speed of the wind is w_g = 1.7 m/s resulting in vertical aircraft RMS velocity of 1.1 m/s. The acceleration reaches peak variations up to 5-6 m/s², over 3x the RMS value. b) The two frames provide 20 second cut-outs of the full simulation data record depicted to show the signal details from the simulator. The correlation of the aircraft velocity with the low frequency of the vertical wind component is clearly seen.

The vertical acceleration characteristics of the B-200, in comparison with the Savannah, are very similar to those of the Dash-8. The ratio of the standard deviation of the two aircraft types to the same turbulence conditions as set up in the simulator:

$$\text{Rho} = \hat{\sigma}_{acc} \text{(B-200)} / \hat{\sigma}_{acc} \text{(Sav)} = 1.29/2.06 = 0.63$$

Thus, the response ratio for the B-200 is only slightly higher than that of the Dash-8 in terms of standard deviations of vertical acceleration or about 68% of that of the Savannah response. The King Air vertical speed response, which is shown in Figs 5-9 a) and b) and Figure 5-10, demonstrate these similarities in more detail.

Response of the Boeing 737 - 9

The Beechcraft B – 737 MAX - 9 and - 8 are now used extensively by Icelandair to replace the B-727 as a mainstay of its fleet. Its turbulence performance is consequently of importance. The turbulence characteristics of the A 320/321 family of aircraft, used by Play Airlines and many other operators flying into and out of Keflavik Airport, are expected to be similar to those of the B 737 under the same conditions.
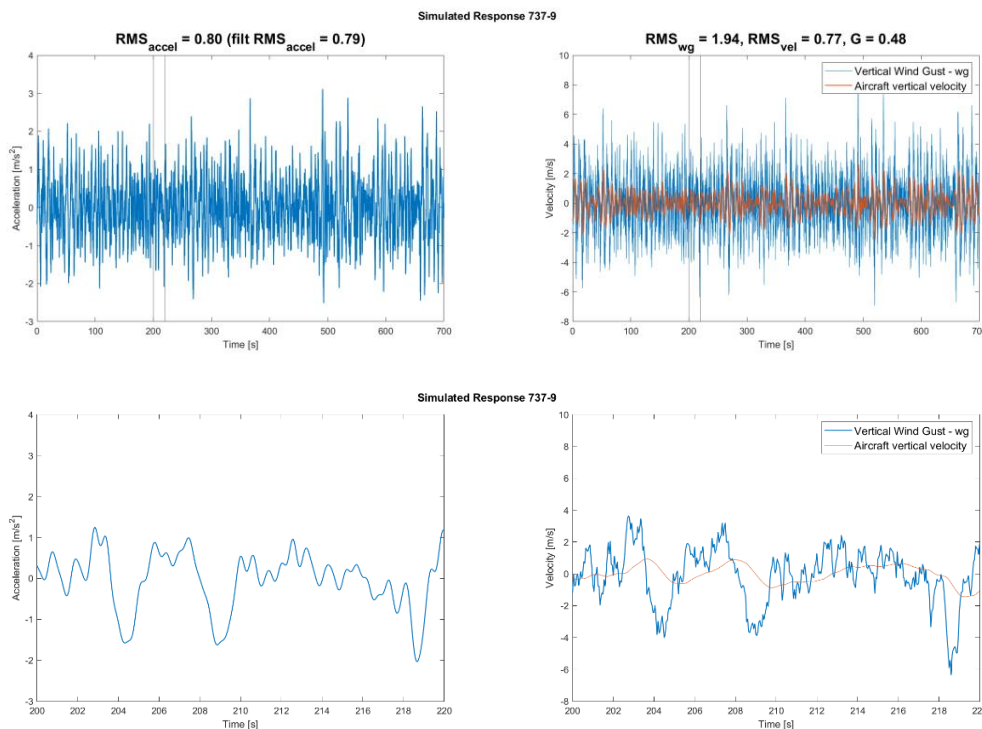

Figure I-2 a) Simulated response of the B-737-9 aircraft at approach airspeed over a 700 second, 50 km flight segment. The vertical wind intensity is set for EDR = 0.4 resulting in vertical acceleration of RMS 0.8 m/s^2. The corresponding RMS vertical speed of the wind is w_g = 1.9 m/s resulting in vertical aircraft RMS velocity of 0.8 m/s. The acceleration reaches peak variations up to 2-3 m/s^2, approximately 3x the RMS value. b) The two frames provide 20 second cut-outs of the full simulation data record depicted to show the signal details from the simulator. The correlation of the aircraft velocity with the low frequency of the vertical wind component is apparent whereas the high frequency is smoothed out.

The ratio of the standard deviation of the two aircraft types to the same turbulence conditions as set up in the simulator:

Rho = $\hat{\sigma}_{acc}$ (737-9) / $\hat{\sigma}_{acc}$ (Sav) = 0.79/2.06 = 0.39

Thus, the response ratio for the B-737-9 is only slightly higher than that of the Dash-8 in terms of standard deviations of vertical acceleration or about 68% of that of the Savannah response. The King Air vertical speed response, which is shown in Figs 5-9 a) and b) and Figure 5-10, demonstrate these similarities in more detail.

EDR estimates of the Test Runs

The EDR estimates that are obtained from the simulation runs of the five types of aircraft by using the simulated acceleration measurements are provided in Figure I-3.
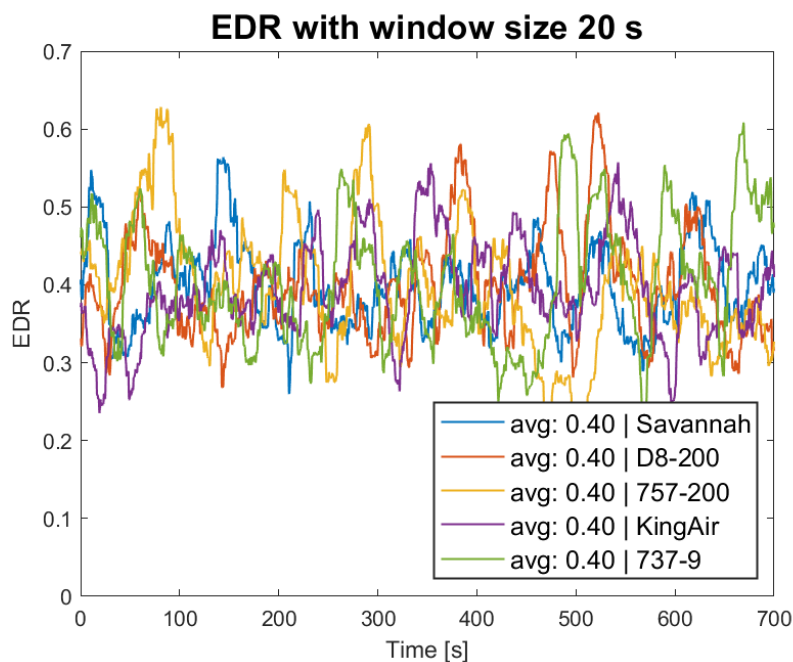

Figure I-3. EDR estimates obtained from simulated acceleration measurements for the five types of aircraft in approach mode of flight.

Although considerable fluctuations are observed in the EDR estimates over the 12-minute period using the 20s RMS window size the simulations all have an average EDR value of 0.4 m$^{2/3}$/s.

I.3   Key Statistical Results of Type Simulation Tests

The results of the tests performed to assess the effect of turbulence on five types of aircraft commonly expected to operate at an airport in Hvassahraun are provided in Table I.2.

Table I.2   Response Characteristics of four types of aircraft to the same average strength of turbulence: mean EDR = 0.4 with $\sigma_{wg} \sim 1.7$ m/s.

EDR = 0.4 $m^{2/3}$/s at typical final approach airspeeds as pr. Table I-1.

Aircraft Type (A/C)	RMS A/C acceleration (m/s^2)	RMS A/C acceleration (BP filtered)	RMS A/C velocity (m/s)	RMS wind vel. (m/s)	Xi* ξ	Zeta** ζ
Savannah	2.09	2.06	1.33	1.53	1.00	0.87
D8-200	0.95	0.94	0.84	1.69	0.46	0.50
King Air 200	1.31	1.29	1.05	1.70	0.63	0.62
B737-9	0.80	0.79	0.77	1.94	0.39	0.40
B757-200	0.73	0.72	0.69	1.80	0.35	0.38

A/C represents the aircraft type.

Response of an aircraft to turbulence is expressed in this project in terms of the standard deviation of the vertical acceleration. This metric captures the most important component of turbulence which is routinely measured in commercial transport aircraft as a vital measure of operational load to analyze individual events as well as long term structural fatigue. In this project it is found convenient to use the ultra-light Savannah aircraft as a reference to express the relative sensitivity of other types of aircraft to turbulence.